ON INNER ITERATIONS OF THE JOINT BIDIAGONALIZATION BASED ALGORITHMS FOR SOLVING LARGE SCALE LINEAR DISCRETE ILL-POSED PROBLEMS *

HAIBO LI†

Abstract. The joint bidiagonalization process of a large matrix pair $\{A, L\}$ can be used to develop iterative regularization algorithms for large scale ill-posed problems in general-form Tikhonov regularization $\min_x \{\|Ax-b\|_2^2+\lambda^2\|Lx\|_2^2\}$ or the essentially equivalent one $\min \|Lx\|_2$ s.t. $x \in \mathcal{S} = \{x|\ \|Ax-b\|_2 \le \eta\|e\|_2\}$, where e is a Gaussian white noise, L is a regularization matrix and $\eta > 1$ slightly. A bottleneck of the algorithms is that a large scale inner least squares problem with $(A^T, L^T)^T$ as the coefficient matrix must be solved at each outer iteration, which may be costly, especially when the solution accuracy of these problems is high. We investigate the solution accuracy requirement on the inner least squares problems and give a reliable stopping tolerance of the LSQR for iteratively solving the inner least squares problems. The results show that the solution accuracy of the inner least squares problems can be relaxed considerably while it will not reduce the accuracy of regularized solutions, thus the overall efficiency of the algorithms can be improved substantially. We also discuss some details for implementing the joint bidiagonalization based regularization algorithms efficiently and stably. Numerical experiments are made to illustrate our results and show some numerical performance of the algorithms.

Key words. ill-posed problem, general-form regularization, joint bidiagonalization, LSQR, solution accuracy, discrete Picard condition, semi-convergence, secant update

AMS subject classifications. 65F10, 65F22, 65F35, 65F50, 65J20

1. Introduction.

In this paper we consider the following linear discrete ill-posed problem

$$\min_{x\in\mathbb{R}^n} \|Ax-b\|_2 \quad or \quad Ax=b, \quad A\in\mathbb{R}^{m\times n}, \tag{1.1}$$

where the matrix A is ill-conditioned with its singular values decaying gradually towards zero without any noticeable gap and the right-hand side $b = b_{true} + e$ is contaminated by a white noise e. Such problems typically arise in connection with the numerical solution of inverse problems. Numerical solution of such kind of problems arise in a broad class of applications such as image deblurring, signal processing, geophysics, computerized tomography, and many others, see [28, 27, 23, 14]. Since A is ill-conditioned, the presence of the noise in b makes that the naive solution $x_{naive} = A^\dagger b$ of (1.1) is a meaningless approximation to the true solution $x_{true} = A^\dagger b_{true}$, where "†" denotes the Moore-Penrose inverse of a matrix. Therefore, it is necessary to use some regularization techniques for finding an acceptable numerical approximation to x_{true} [11, 13].

Throughout the paper we assume that $Ax_{true} = b_{true}$ and $m \ge n$. A well-known and highly regarded regularization method is the Tikhonov regularization. In particular, the *general-form Tikhonov regularization* corresponds to defining a regularized solution x_λ by

$$x_\lambda = \arg\min_{x\in\mathbb{R}^n} \{\|Ax-b\|_2^2+\lambda^2\|Lx\|_2^2\}, \tag{1.2}$$

where L is a $p\times n$ regularization matrix which defines the smoothing term $\|Lx\|_2$, and $\lambda > 0$ is called the *regularization parameter*. Another regularization approach which

*This work was supported in part by the National Science Foundation of China (No. 11771249)

†Department of Mathematical Sciences, Tsinghua University, 100084 Beijing, China. (li-hb15@mails.tsinghua.edu.cn)

is essentially equivalent to (1.2) is the following *general-form regularization*

$$\min \|Lx\|_2 \quad \text{s.t.} \quad x \in \mathcal{S} = \{x| \ \|Ax - b\|_2 \leq \eta \|e\|_2\} \tag{1.3}$$

with some $\eta > 1$. The matrix L is problem dependent, and typical choices for L include (scaled) discrete first or second derivative operators in the appropriate dimension [11, 13]. If $L = I_n$, the $n \times n$ identity matrix, then (1.2) and (1.3) are called *standard-form regularization problems*. We assume that $\begin{pmatrix} A \\ L \end{pmatrix}$ has full rank such that the null spaces of A and L intersect trivially and the solution x_λ to (1.2) is unique. If λ and L are chosen appropriately, the regularized solution should approximate the desired solution x_{true}.

For large scale problems, x_λ is usually computed by applying an iterative least squares method to (1.2), such as CGLS or LSQR [2, 30]. However, this approach is computationally very demanding if the regularization parameter is not known a priori, and many different values of λ must be tried. For large scale problems, an alternative is the *iterative regularization* method. In this case, an iterative method such as LSQR projects (1.1) onto a sequence of lower-dimensional subspaces, and then solves the projected small scale problems. Finally the solution is transformed back to the original domain to approximate x_{true}, [2, 3]. This approach usually exhibits semi-convergence: at early iterations solutions converge to x_{true} while afterwards the noise e starts to deteriorate the solutions so that they start to diverge from x_{true} and instead converge to x_{naive}. If we stop iterations at the right time, then, in principle, we will have a good regularization solution, where the iteration number plays the role of the regularization parameter [17, 18]. The semi-convergence behavior of LSQR can be stabilized by using a *hybrid method*, eg., [29, 4, 31, 5], where the Tikhonov regularization combined with a parameter-choice method is applied to the projected problem [25, 32].

The common approach to treating the general case with $L \neq I_n$, is to use a standard-form transformation. If L is invertible, then we can use the substitution $y = Lx$. Otherwise, (1.2) and (1.3) can be transformed to their standard forms with $L = I_n$ and A replaced by $AL_A^\dagger$, where $L_A^\dagger = (I - (A(I - L^\dagger L))^\dagger A)L^\dagger$ is the *A-weighted pseudoinverse of* L and $L_A^\dagger = L^\dagger$ when $p \geq n$, see [7, 11] for details. This is computationally viable and attractive if not much effort is needed by applying $L_A^\dagger$, e.g., when L is banded with small bandwidth and has a known null space, [5, 6]. However, such transformation is computationally unfeasible in many practical applications. Therefore we are interested in alternative projection-based approaches based on suited Krylov subspaces and avoid the use of $L_A^\dagger$.

Recently, there have been some available iterative algorithms for solving the regularization problem (1.2) or (1.3) when applying $L_A^\dagger$ is computationally unfeasible. For example, Jia and Yang [22] have developed efficient randomized SVD algorithms for solving (1.3) effectively. Inspired by a bidiagonalization algorithm by Zha [34] for computing dominant generalized singular values and vectors of the matrix pair $\{A, L\}$, Kilmer *et al.* [24] developed a joint bidiagonalization process that successively reduces the matrix pair $\{A, L\}$ to lower and upper bidiagonal forms, based on which they proposed a hybrid projection method for solving (1.2). Based on the joint bidiagonalization process, instead of developing any hybrid algorithms, Jia and Yang [21] proposed a pure iterative projection algorithm for solving (1.3) other than the equivalent (1.2), which is much simpler than the hybrid one in [24], and the iteration number plays the role of the regularization parameter.

The joint bidiagonalization based algorithms produce legitimate solution subspaces for general-form regularization, which can be illuminated in two aspects: (i) the generalized right singular vectors of the matrix pair $\{A, L\}$ form a more suitable basis to express a regularized solution [24, 21]; (ii) the joint bidiagonalization process tends to capture the dominant generalized singular value decomposition(GSVD) components of the matrix pair $\{A, L\}$ while suppress those corresponding to small generalized singular values [24, 26]. For $L = I_n$ and the LSQR, it has been proved by Jia [17, 18, 19] that for severely ill-posed problems and some moderately ill-posed ones the singular values of the matrices involved in the projected problems approximate the large singular values of A in natural order, thus the LSQR has *full regularization* effect on these kind of ill-posed problems. For the definition of severely, moderately and mildly ill-posed problems, see [11, 13]. An adaption of this result to $L \neq I_n$ says that if the above sufficient conditions are met, the pure iterative projection algorithm resembles the truncated GSVD (TGSVD) method [11] until the occurrence of semi-convergence and the best regularized solution is as accurate as the best TGSVD solution, which is a best regularized solution to (1.1) in the sense of the regularization formulation (1.3).

At each iteration of the joint bidiagobalization process, a large scale linear least squares problem with the coefficient matrix $(A^T, L^T)^T$ is needed to be solved, which is called inner iteration. Fortunately, $(A^T, L^T)^T$ is typically well conditioned as L is typically so in applications [11, 13], and the LSQR algorithm can solve the inner least squares problems iteratively. A bottleneck of the hybrid algorithm and the pure iterative one is that we need to solve a large scale least squares problem at each outer iteration, which may be costly, especially when the solution accuracy of these problems is high. If the inner least squares problem could be solved with considerably relaxed accuracy, we shall gain much, and the overall efficiency of the algorithm can be improved substantially.

In this paper, we investigate the solution accuracy requirement on the inner least squares problem of the joint bidiagonalization based algorithms for solving ill-posed problems. Since b is contaminated by the noise e, even with regularization, we can never achieve an error in the reconstruction which is as small as the $\|e\|_2$. Therefore the accuracy of the best regularized solution will not increase even if the solution accuracy of the inner least squares problems is too high, which comes only at the cost of increasing extra computation. On the other hand, if the solution accuracy is too low, the best regularized solution will be less accurate than the ideal one in exact arithmetic. We use the LSQR algorithm to solve the inner least squares problems iteratively with a given tolerance τ as stopping criterion. Considering the solution accuracy τ and rounding errors, we will investigate the numerical behavior of the joint bidiagonalization process. We mention that the orthogonality of Lanczos vectors obtained by the joint bidiagonalization process quickly lost due to inexactly solving the inner least squares problems and the presence of rounding errors [26], which slows down the convergence of regularized solutions. Therefore, the joint bidiagobalization process is performed with full reorthogonalization of the computed Lanczos vectors to ensure preserving their orthogonality close to machine precision. We will investigate how the accuracy of the regularized solutions be influenced by the solution accuracy of the inner least squares problem. Our results give a reliable choice of τ, which dependent on $\|b\|_2$ and $\|e\|_2$, as stopping tolerance of the LSQR for solving the inner least squares problems. Therefore, the solution accuracy of the inner least squares problem can be relaxed considerably while it not reduce the accuracy of regularized solutions.

We also discuss some implementation details of the two joint bidiagonalization based regularization algorithms, which have not been investigated carefully in [24, 21]. For the hybrid algorithm, we discuss some methods for choosing regularization parameters of the projected problems at each iteration, while for the pure iterative algorithm, we give a procedure to update regularized solutions step by step efficiently and discuss some methods for terminating iterations at the right time.

The paper is organized as follows. In Section 2, we overview some background, including the joint bidiagonalization, the GSVD, and the joint bidiagonalization based regularization algorithms proposed in [25, 21]. In Section 3, we investigate the solution accuracy of the inner least squares problem in the joint bidiagonalization, and give some results about the numerical behaviors of the joint bidiagonalization. In Section 4, we analyze how the accuracy of the regularized solutions be influenced by the solution accuracy τ of the inner least squares problem. Based on the discrete Picard condition, we give a reliable choice of τ, with which the joint bidiagonalization based regularization algorithms can obtain regularized solutions with the same accuracy as the ideal one in exact arithmetic. In Section 5, we discuss the estimation of the optimal regularization parameters and efficient methods to update solutions step by step. In Section 6, we use some test problems to illustrate our results, and show some numerical performance of the joint bidiagonalization based regularization algorithms. Finally, we conclude the paper in Section (7).

Throughout the paper, we denote by $\mathcal{K}_k(C, w) = span\{w, Cw, \ldots, C^{k-1}w\}$ the k dimensional Krylov subspace generated by the matrix C and vector w, and by 0_l and $0_{l\times k}$ the l-dimension zero column vector and zero matrix of order $l \times k$, respectively. The transpose of a matrix C is denoted by C^T. The roundoff unit is denoted by ϵ. The norm $\|\cdot\|$ always means the spectral or 2-norm of a matrix or vector.

2. Background.

In this section, we provide some necessary background. We describe the joint bidiagonalization process, the GSVD and regularization of ill-posed problems. We also review the two joint bidiagonalization based regularization algorithms proposed in [24] and [21].

2.1. Joint bidiagonalization.

Consider the compact QR factorization of the stacked matrix:

$$\begin{pmatrix} A \\ L \end{pmatrix} = QR = \begin{pmatrix} Q_A \\ Q_L \end{pmatrix} R, \tag{2.1}$$

where $Q \in \mathbb{R}^{(m+p)\times n}$ is column orthonormal and $R \in \mathbb{R}^{n\times n}$. We partition Q such that $Q_A \in \mathbb{R}^{m\times n}$ and $Q_L \in \mathbb{R}^{p\times n}$, and we have $A = Q_A R$ and $L = Q_L R$. Following the assumption that $(A^T, L^T)^T$ is of full column rank, $R \in \mathbb{R}^{n\times n}$ is upper triangular and nonsingular.

Applying the BIDIAG-1 algorithm and BIDIAG-2 algorithm [30], which correspond to the lower and upper Lanczos bidiagonalization processes, of Q_A and Q_L, respectively, we can reduce Q_A and Q_L to the following lower and upper bidiagonal matrices respectively:

(2.2)

$$B_k = \begin{pmatrix} \alpha_1 & & & \\ \beta_2 & \alpha_2 & & \\ & \beta_3 & \ddots & \\ & & \ddots & \alpha_k \\ & & & \beta_{k+1} \end{pmatrix} \in \mathbb{R}^{(k+1)\times k}, \quad \widehat{B}_k = \begin{pmatrix} \hat{\alpha}_1 & \hat{\beta}_1 & & \\ & \hat{\alpha}_2 & \ddots & \\ & & \ddots & \hat{\beta}_{k-1} \\ & & & \hat{\alpha}_k \end{pmatrix} \in \mathbb{R}^{k\times k}.$$

The two processes can be written in matrix form:

$$Q_A V_k = U_{k+1} B_k, \quad Q_A^T U_{k+1} = V_k B_k^T + \alpha_{k+1} v_{k+1} e_{k+1}^T, \tag{2.3}$$

$$Q_L \widehat{V}_k = \widehat{U}_k \widehat{B}_k, \quad Q_L^T \widehat{U}_k = \widehat{V}_k \widehat{B}_k^T + \hat{\beta}_k \hat{v}_{k+1} e_k^T, \tag{2.4}$$

where e_{k+1} and e_k are the $(k+1)$-th and k-th canonical vectors of dimensions $k+1$ and k, respectively, and

$$U_{k+1} = (u_1, \ldots, u_{k+1}) \in \mathbb{R}^{m \times (k+1)}, \quad \widehat{U}_k = (\hat{u}_1, \ldots \hat{u}_k) \in \mathbb{R}^{p \times k}, \tag{2.5}$$

$$V_k = (v_1, \ldots, v_k) \in \mathbb{R}^{n \times k}, \quad \widehat{V}_k = (\hat{v}_1, \ldots, \hat{v}_k) \in \mathbb{R}^{n \times k} \tag{2.6}$$

are column orthonormal.

In order to join BIDIAG-1 and BIDIAG-2, we choose the starting vector of BIDIAG-2 to be $\hat{v}_1 = v_1$ and continue the upper bidiagonalization process, then in exact arithmetic we have

$$\hat{v}_{i+1} = (-1)^i v_{i+1}, \quad \hat{\alpha}_i \hat{\beta}_i = \alpha_{i+1} \beta_{i+1},$$

which has been proved in [34, 24]. For large scale matrices A and L, the explicitly QR factorization (1.1) can be avoided by solving a least squares problem with $(A^T, L^T)^T$ as the coefficient matrix iteratively at each iteration. This is summarized in Algorithm 1.

Algorithm 1 The k-step joint bidiagonalization(JBD) process

1: Choosing a starting vector $b \in \mathbb{R}^m$, $\beta_1 u_1 = b$, $\beta_1 = \| b \|$
2: $\alpha_1 \tilde{v}_1 = QQ^T \begin{pmatrix} u_1 \\ 0_p \end{pmatrix}$
3: $\hat{\alpha}_1 \hat{u}_1 = \tilde{v}_1(m+1 : m+p)$
4: **for** $i = 1, 2, \ldots, k$, **do**
5: $\quad \beta_{i+1} u_{i+1} = \tilde{v}_i(1 : m) - \alpha_i u_i$
6: $\quad \alpha_{i+1} \tilde{v}_{i+1} = QQ^T \begin{pmatrix} u_{i+1} \\ 0_p \end{pmatrix} - \beta_{i+1} \tilde{v}_i$
7: $\quad \hat{\beta}_i = (\alpha_{i+1} \beta_{i+1}) / \hat{\alpha}_i$
8: $\quad \hat{\alpha}_{i+1} \hat{u}_{i+1} = (-1)^i \tilde{v}_{i+1}(m+1 : m+p) - \hat{\beta}_i \hat{u}_i$
9: **end for**

In exact arithmetic, the k-step JBD process computes the lower bidiagonal matrix B_k and upper bidiagonal matrix $\widehat{B}_k$, as well as three column orthonormal matrices U_{k+1}, $\widehat{U}_k$ and

$$\widetilde{V}_k = (\tilde{v}_1, \cdots, \tilde{v}_k) \in \mathbb{R}^{n \times k} \tag{2.7}$$

satisfying $\tilde{v}_i = Q v_i$. The k-step JBD process can be written in matrix form:

$$(I_m, 0_{m \times p}) \widetilde{V}_k = U_{k+1} B_k, \tag{2.8}$$

$$QQ^T \begin{pmatrix} U_{k+1} \\ 0_{p \times (k+1)} \end{pmatrix} = \widetilde{V}_k B_k^T + \alpha_{k+1} \tilde{v}_{k+1} e_{k+1}^T, \tag{2.9}$$

$$(0_{p \times m}, I_p) \widetilde{V}_k P = \widehat{U}_k \widehat{B}_k, \tag{2.10}$$

where $P = diag(1, -1, 1, \ldots, (-1)^{k-1})_{k \times k}$.

At each iteration $i = 1, 2, \ldots, k+1$, Algorithm 1 needs to compute $QQ^T \begin{pmatrix} u_i \\ 0_p \end{pmatrix}$, which is not accessible since Q is not available. Let $\tilde{u}_i = \begin{pmatrix} u_i \\ 0_p \end{pmatrix}$. Notice that $QQ^T\tilde{u}_i$ is nothing but the orthogonal projection of $\tilde{u}_i$ onto the column space of $\begin{pmatrix} A \\ L \end{pmatrix}$, which means that $QQ^T\tilde{u}_i = \begin{pmatrix} A \\ L \end{pmatrix} \tilde{x}_i$, where

$$\tilde{x}_i = \arg\min_{\tilde{x}\in\mathbb{R}^n} \left\| \begin{pmatrix} A \\ L \end{pmatrix} \tilde{x} - \tilde{u}_i \right\|. \tag{2.11}$$

Since the least squares problem is large scale, it is generally only feasible to solve it by an iterative algorithm. The computation of (2.11) is called the *inner iteration* of the JBD process. Here we use the LSQR algorithm to solve the inner least squares problems (2.11) with a given tolerance τ as stopping criterion, for details see [30].

2.2. GSVD and regularization. Following (2.1), let

$$Q_A = P_A C_A H^T, \quad Q_L = P_L S_L H^T \tag{2.12}$$

be the CS decomposition of the matrix pair $\{Q_A, Q_L\}$ [10], where $P_A \in \mathbb{R}^{m\times m}$, $P_L \in \mathbb{R}^{p\times p}$ and $H \in \mathbb{R}^{n\times n}$ are orthogonal matrices, and $C_A \in \mathbb{R}^{m\times n}$ and $S_L \in \mathbb{R}^{p\times n}$ are diagonal matrices(not necessarily square) satisfying $C_A^T C_A + S_L^T S_L = I_n$. Then the GSVD of $\{A, L\}$ is

$$A = P_A C_A G^{-1}, \quad L = P_L S_L G^{-1} \tag{2.13}$$

with $G = R^{-1}H = (g_1, g_2, \ldots, g_n) \in \mathbb{R}^{n\times n}$, where the invertibility of G follows from the assumption that $(A^T, L^T)^T$ has full rank and the vectors g_i are the generalized right singular vectors of $\{A, L\}$. Following [24], we order the entries of the diagonal matrices C_A and S_L so that

$$1 \geq c_1 \geq \cdots \geq c_{\min\{n,p\}} \geq 0, \quad c_{\min\{n,p\}+1} = \cdots = c_n = 1, \tag{2.14}$$

$$0 \leq s_1 \leq \cdots \leq s_{\min\{n,p\}} \leq 1, \tag{2.15}$$

then the generalized singular values of $\{A, L\}$ are $\gamma_i = c_i/s_i$, which appear in nonincreasing order similar to the standard SVD.

The *discrete Picard condition(DPC)* plays a central role in connection with discrete ill-posed problems, which says that the Fourier coefficients $|p_{i,A}^T b^{true}|$ on average decay to zero faster than the conresponging γ_i, where $P_A = (p_{1,A}, p_{2,A}, \ldots, p_{m,A})$. It is well known from, e.g. [11, 13], that any regularization is based on an underlying requirement that the DPC for a given problem is satisfied, only under which can one compute a useful regularized solution with some accuracy. If, on the other hand, the given problem does not satisfy the DPC, then it is generally not possible to compute a satisfactory solution by means of Tikhonov regularization or any related methods. Throughout the rest of the paper, we assume that the DPC is satisfied.

Using the GSVD of $\{A, L\}$, the general-form Tikhonov solution to (1.2) takes a filtered GSVD expansion:

$$\begin{aligned} x_\lambda &= (A^TA + \lambda^2 L^TL)^{-1}A^Tb = G(C_A^TC_A + \lambda^2 S_L^TS_L)^{-1}C_A^TP_A^Tb \\ &= \sum_{i=1}^{\min\{n,p\}} \frac{c_i^2}{c_i^2 + \lambda^2 s_i^2} \frac{p_{i,A}^T b}{c_i} g_i + \sum_{i=\min\{n,p\}+1}^{n} (p_{i,A}^T b) g_i, \end{aligned} \tag{2.16}$$

where $f_i = \frac{c_i^2}{c_i^2+\lambda^2 s_i^2}$ are filters. We mention that the second term which lies in the null space of L are not influenced by the regularization.

As comparison, we also give the k-th TGSVD solution

$$x_k^{tgsvd} = \sum_{i=1}^{k} \frac{p_{i,A}^T b}{c_i} g_i + \sum_{i=\min\{n,p\}+1}^{n} (p_{i,A}^T b) g_i, \quad k = 1, 2, \ldots, \min\{n, p\}, \tag{2.17}$$

where the first term consists of the first k dominant GSVD components of $\{A, L\}$, and the number k plays the role of the regularization parameter.

2.3. Joint bidiagonalization based regularization methods. In exact arithmetic, one can obtain from (2.3) and (2.4) that the k-step JBD process satisfies

$$AZ_k = U_{k+1} B_k, \quad LZ_k = \widehat{U}_k \bar{B}_k, \tag{2.18}$$

where $Z_k = R^{-1} V_k = (z_1, \ldots, z_k)$ and $\bar{B}_k = \widehat{B}_k P$. Therefore, one can use the k-step JBD process to approximate the dominant GSVD components of $\{A, L\}$ by the SVD of B_k or $\bar{B}_k$, for details see [34, 26]. The property of capturing the dominant GSVD components of $\{A, L\}$ makes the JBD process a potential regularization methods for ill-posed problems. We review the two JBD based regularization methods: the hybrid projection method in [24] and the pure iterative projection method in [21].

For a given regularization parameter λ, the hybrid projection method seeks the solution $x_k^\lambda \in \mathcal{R}(Z_k)$ such that

$$x_k^\lambda = \arg \min_{x \in \mathcal{R}(Z_k)} \{\|Ax - b\|^2 + \lambda^2 \|Lx\|^2\}, \quad \mathcal{R}(Z_k) = \text{span}\{z_1, \ldots, z_k\}. \tag{2.19}$$

Notice that $U_{k+1}(\beta_1 e_1) = b, \beta_1 = \|b\|$, where e_1 is the first canonical vector of dimension $k+1$. Write $x_k^\lambda = Z_k y_k^\lambda$ and using (2.18) we have

$$\begin{aligned} \|Ax_k^\lambda - b\|^2 + \lambda^2 \|Lx_k^\lambda\|^2 &= \|AZ_k y_k^\lambda - U_{k+1}\beta_1 e_1\|_2 + \lambda^2 \|LZ_k y_k^\lambda\|^2 \\ &= \|B_k y_k^\lambda - \beta_1 e_1\|^2 + \lambda^2 \|\bar{B}_k y_k^\lambda\|^2 \end{aligned}$$

Therefore, at iteration k the hybrid projection method solves a projected general-form Tikhonov regularization problem

$$\min_y \{\|B_k y - \beta_1 e_1\|^2 + \mu_k^2 \|\bar{B}_k y\|^2\}, \tag{2.20}$$

where the new notation $\mu_k > 0$ is introduced to specialize the regularization parameter for the projected problem at iteration k. The main idea is that once k is large enough, the projected problem will capture the main features/components of the original problem. Let λ^{opt} and μ_k^{opt} denote the optimal regularization parameters of the original problem (1.2) and projected problem (2.20) respectively. Then there is good hope that, for large enough k, μ_k^{opt} converges to λ^{opt} and the corresponding solution $x_{\mu_k^{opt}}$ to (2.19) will be a good approximation to $x_{\lambda^{opt}}$.

Instead of solving (1.2), the pure iterative projection method solves (1.3), where the iteration number k plays the role of the regularization parameter. Specifically, we seek $x_k = Z_k y_k \in \mathcal{R}(Z_k)$ by solving the reduced general-form regularization problem

$$\min \|LZ_k y\| \quad \text{s.t.} \quad y \in \{y | \ \|AZ_k y - b\| = \min\} \tag{2.21}$$

for y_k, starting with $k = 1$ onwards. Using (2.18), (2.21) becomes the projected general-form regularization problem

$$\min \|\bar{B}_k y\| \quad \text{s.t.} \quad y \in \{y| \ \|B_k y - \beta_1 e_1\| = \min\}\,. \tag{2.22}$$

Assume that Algorithm 1 does not break down at iteration $k \leq \min\{n, p\}$. Since B_k is of column full rank, the solution to (2.22) is

$$y_k = \arg\min_{y\in\mathbb{R}^k} ||B_k y - \beta_1 e_1|| = \beta_1 B_k^{\dagger} e_1, \tag{2.23}$$

which is simply the solution to the ordinary least squares problem $\min_y ||B_k y - \beta_1 e_1||$ and $\bar{B}_k$ is not invoked. The algorithm has the typical semi-convergence property: as the joint bidiagonalization process proceeds, more and more dominant generalized singular components of $\{A, L\}$ are captured, and the regularized solutions converge to the true solution x_{true} of (1.1) until some iteration, after which the regularized solutions start to be deteriorated by the noise e and instead converge to x_{naive}. We can use the L-curve criterion or the discrepancy principle to estimate the optimal k_0, at which the semi-convergence occurs.

One only needs to form x_k^{λ} or x_k explicitly when it is accepted as the final regularized solution. Since

$$\begin{pmatrix} A \\ L \end{pmatrix} Z_k = QR(R^{-1}V_k) = QV_k = \widetilde{V}_k,$$

it follows that x_k^{λ} and x_k satisfy

$$\begin{pmatrix} A \\ L \end{pmatrix} x_k^{\lambda} = \widetilde{V}_k y_k^{\lambda}, \quad \begin{pmatrix} A \\ L \end{pmatrix} x_k = \widetilde{V}_k y_k, \tag{2.24}$$

respectively, which can be computed iteratively by means of CGLS or LSQR.

3. Inner iteration of the joint bidiagonalization. In this section we investigate the solution accuracy requirement on the inner least squares problems (2.11). Our analysis also considers rounding errors at each iteration of the JBD process, while other operations are all assumed to be performed in exact arithmetic. Besides, we assume that the JBD process does not break down at step $i < \min\{n, p\}$. We change the notations a bit, to denote the quantities generated by the JBD process in exact arithmetic by adding "*" as superscript, such as B_k^*, $\widehat{B}_k^*$, x_k^* and so on, while the corresponding computed versions are B_k, $\widehat{B}_k$, x_k and so on. The Lanczos vectors u_i, $\tilde{v}_i$ and $\hat{u}_i$ are assumed to be unitary.

We investigate the computation of the inner iteration (2.11) by using the LSQR algorithm with tolerance τ as stopping criterion, which means

$$\frac{\|Z^T \bar{r}_i\|}{\|Z\|\|\bar{r}_i\|} \leq \tau,$$

where $Z = \begin{pmatrix} A \\ L \end{pmatrix}$, $\bar{x}_i$ is the computed version of $\tilde{x}_i$, and the residual is $\bar{r}_i = \tilde{u}_i - Z\bar{x}_i$. It is known from [30] that the computed $\bar{x}_i$ is the exact solution to the perturbed problem

$$\min_x \|\tilde{u}_i - (Z + E_i)x\|, \tag{3.1}$$

where

$$E_i = -\frac{\bar{r}_i^T \bar{r}_i Z}{\|\bar{r}_i\|^2}, \quad \frac{\|E_i\|}{\|Z\|} = \frac{\|Z^T \bar{r}_i\|}{\|Z\|\|\bar{r}_i\|} \le \tau.$$

Suppose that the exact solution of (2.11) is $\tilde{x}_i$ with residual $\tilde{r}_i = \tilde{u}_i - Z\tilde{x}_i$, and the residual of (3.1) is $\tilde{s}_i = \tilde{u}_i - (Z + E_i)\bar{x}_i$. Using the perturbation theory of least squares problem [15, Chapter 20], we have

$$\frac{\|\tilde{x}_i - \bar{x}_i\|}{\|\tilde{x}_i\|} \le \frac{\kappa_2(Z)\tau}{1 - \kappa_2(Z)\tau}\Big(2 + \frac{\kappa_2(Z)\|\tilde{r}_i\|}{\|Z\|\|\tilde{x}_i\|}\Big), \tag{3.2}$$

$$\|\tilde{r}_i - \tilde{s}_i\| \le 2\kappa_2(Z)\|\tilde{u}_i\|\tau = 2\kappa_2(Z)\tau \tag{3.3}$$

if $\kappa_2(Z)\tau < 1$, where $\kappa_2(Z) = \|Z\|\|Z^\dagger\|$ is the condition number of Z. Therefore,

$$\begin{aligned} \| Z\tilde{x}_i - Z\bar{x}_i \| &= \| E_i\bar{x}_i - (\tilde{r}_i - \tilde{s}_i) \| \\ &\le \| E_i \|\| \bar{x}_i \| + \| \tilde{r}_i - \tilde{s}_i \| \\ &\le (\| Z \|\| \bar{x}_i \| + 2\kappa_2(Z))\tau \ . \end{aligned} \tag{3.4}$$

Throughout the rest of the paper, we assume that A and L have been scaled so that Z is well conditioned, which is true provided that L is well conditioned, as is usually the case in practical applications. It follows from (3.2) that both $\tilde{x}_i = Z^\dagger\tilde{u}_i$ and $\bar{x}_i$ are two moderate numbers. Notice that the computed version of $QQ^T\tilde{u}_i$ is $Z\bar{x}_i$ instead of the exact one $Z\tilde{x}_i$. Denote $(\|Z\|\|\bar{x}_i\|+2\kappa_2(Z))$ by c_i, which is a moderate number. From (3.4), at the i-th iteration we have

$$\alpha_{i+1}\tilde{v}_{i+1} = QQ^T\begin{pmatrix} u_{i+1} \\ 0_p \end{pmatrix} - \beta_{i+1}\tilde{v}_i - \tilde{g}_{i+1}, \tag{3.5}$$

where $\|\tilde{g}_{i+1}\| \le c_{i+1}\tau$. We mention that here all quantities except Q are computed versions. Considering rounding errors at each iteration of the JBD process, we have the matrix form relations

$$(I_m, 0_{m\times p})\widetilde{V}_k = U_{k+1}B_k + \widetilde{F}_k, \tag{3.6}$$

$$QQ^T\begin{pmatrix} U_{k+1} \\ 0_{p\times(k+1)} \end{pmatrix} = \widetilde{V}_k B_k^T + \alpha_{k+1}\tilde{v}_{k+1}e_{k+1}^T + \widetilde{G}_{k+1}, \tag{3.7}$$

where $\widetilde{F}_k = (\tilde{f}_1, \ldots, \tilde{f}_k)$, $\widetilde{G}_{k+1} = (\tilde{g}_1, \ldots, \tilde{g}_{k+1})$, and $\|\tilde{f}_i\| = O(\epsilon)$, $\|\tilde{g}_i\| \le c_i\tau$. Notice that $Z\bar{x}_i$ is the computed version of $QQ^T\tilde{u}_i$, so (3.5) have another form

$$\alpha_{i+1}\tilde{v}_{i+1} = Z\bar{x}_i - \beta_{i+1}\tilde{v}_i - \bar{g}_{i+1},$$

where $\|\bar{g}_{i+1}\| = O(\epsilon)$ is rounding errors in the computations. Equating the first k terms yields

$$Z\bar{X}_k = \widetilde{V}_k\underline{B}_k + \bar{G}_k,$$

where $\underline{B}_k = \begin{pmatrix} B_{k-1}^T \\ \alpha_k e_k^T \end{pmatrix} \in \mathbb{R}^{k\times k}$, $\bar{X}_k = (\bar{x}_1, \ldots, \bar{x}_k)$ and $\bar{G}_k = (\bar{g}_1, \ldots, \bar{g}_k)$. Let $v_i = Q^T\tilde{v}_i$ and $V_k = (v_1, \ldots, v_k) = Q^T\widetilde{V}_k$. Since $\widetilde{V}_k = Z\bar{X}_k\underline{B}_k^{-1} - \bar{G}_k\underline{B}_k^{-1}$, we have

$$\widetilde{V}_k - QV_k = \widetilde{V}_k - QQ^TQR\bar{X}_k\underline{B}_k^{-1} + QQ^T\bar{G}_k\underline{B}_k^{-1} = (QQ^T - I_{m+p})\bar{G}_k\underline{B}_k^{-1},$$

and thus

$$\|\widetilde{V}_k - QV_k\| \leq \|\bar{G}_k \underline{B}_k^{-1}\| = O(\|\underline{B}_k^{-1}\|\epsilon). \tag{3.8}$$

We can rewrite (3.6) as

$$(I_m, 0_{m\times p})QV_k = U_{k+1}B_k + F_k, \tag{3.9}$$

where $F_k = \widetilde{F}_k - (I_m, 0_{m\times p})(\widetilde{V}_k - QV_k) = O(\|\underline{B}_k^{-1}\|\epsilon)$. Premultiply (3.7) by Q^T and combine with (3.9), we have the following result.

THEOREM 3.1. *Suppose the inner iteration (2.11) of the k-step JBD process is solved by the LSQR algorithm with tolerance τ as stopping criterion. In finite precision arithmetic it follows*

$$Q_A V_k = U_{k+1}B_k + F_k, \tag{3.10}$$

$$Q_A^T U_{k+1} = V_k B_k^T + \alpha_{k+1} v_{k+1} e_{k+1}^T + G_{k+1}, \tag{3.11}$$

where $F_k = (f_1, \ldots, f_k)$, $G_{k+1} = (g_1, \ldots, g_{k+1}) = Q^T \widetilde{G}_{k+1}$, and $\|F_k\| = O(\|\underline{B}_k^{-1}\|\epsilon)$, $\|G_{k+1}\| = O(\tau)$.

By Theorem 3.1, we can treat the process of computing U_{k+1}, V_k and B_k as the k-step (lower) Lanczos bidiagonalization process of Q_A with rounding errors $O(\|\underline{B}_k^{-1}\|\epsilon)$ or $O(\tau)$ at each step. Due to the influence of rounding errors, the orthogonality of Lanczos vectors u_i and $\tilde{v}_i$ will be gradually lost, which causes that the convergence of some approximate GSVD components can be significantly delayed [26]. Let $\mathbf{SUT}(\cdot)$ denotes the strictly upper triangular part of a matrix, the orthogonal levels of U_{k+1} and $\widetilde{V}_k$ can be measured as

$$\mu_{k+1} = \|\mathbf{SUT}(I_{k+1} - U_{k+1}^T U_{k+1})\|, \quad \tilde{\nu}_k = \|\mathbf{SUT}(I_k - \widetilde{V}_k^T \widetilde{V}_k)\|$$

respectively. Since

$$\begin{aligned}
\widetilde{V}_k^T (I_{m+p} - QQ^T)\widetilde{V}_k &= \widetilde{V}_k^T (\widetilde{V}_k - QV_k) = \widetilde{V}_k^T (QQ^T - I_{m+p})\bar{G}_k \underline{B}_k^{-1} \\
&= -[(I_{m+p} - QQ^T)\widetilde{V}_k]^T \bar{G}_k \underline{B}_k^{-1} \\
&= \underline{B}_k^{-T} \bar{G}_k^T (I_{m+p} - QQ^T)\bar{G}_k \underline{B}_k^{-1},
\end{aligned}$$

we have

$$\begin{aligned}
I_k - V_k^T V_k &= I_k - \widetilde{V}_k^T QQ^T \widetilde{V}_k = I_k - \widetilde{V}_k^T \widetilde{V}_k + \widetilde{V}_k^T (I_{m+p} - QQ^T)\widetilde{V}_k \\
&= (I_k - \widetilde{V}_k^T \widetilde{V}_k) + \underline{B}_k^{-T} \bar{G}_k^T (I_{m+p} - QQ^T)\bar{G}_k \underline{B}_k^{-1}.
\end{aligned} \tag{3.12}$$

Let

$$\nu_k = \|\mathbf{SUT}(I_k - V_k^T V_k)\|$$

be the orthogonal level of V_k, then from (3.12) we have

$$|\nu_k - \tilde{\nu}_k| \leq \|\underline{B}_k^{-T} \bar{G}_k^T\| \|\bar{G}_k \underline{B}_k^{-1}\| = O(\|\underline{B}_k^{-1}\|^2 \epsilon^2).$$

For solving large scale ill-posed problems, it will not take too many iterations to get a desired regularized solution, thus $\|\underline{B}_k^{-1}\|$ is usually not too big and thus $\|\underline{B}_k^{-1}\|\epsilon \ll \tau$

and $|\nu_k - \tilde{\nu}_k| = O(\tau^2)$ or even $|\nu_k - \tilde{\nu}_k| = O(\epsilon)$. In the following analysis, we always assume that

$$\|\underline{B}_k^{-1}\|\epsilon \ll \tau, \quad |\nu_k - \tilde{\nu}_k| = O(\epsilon) \tag{3.13}$$

before we stop the iterations. We will illustrate this by some numerical examples later.

The loss of orthogonality are sometimes acknowledged as a potential difficulty for regularizing ill-posed problems, for it affects convergence of the regularized solutions and makes the propagation of the noise in the bidiagonalization process rather irregular [16]. Therefore, we perform the JBD process with full reorthogonalization of u_i, $\hat{u}_i$ and $\tilde{v}_i$ to ensure preserving orthogonality close to machine precision. Combining with Theorem 3.1 and using the results of backward analysis of the Lanczos bidiagonalization with reorthogonalization in [20, Theorem 4.2], we have the following result.

THEOREM 3.2. *Assume $\mu_{k+1} < 1/2$ and $\nu_k < 1/2$. There exist left orthogonal matrices $\bar{U}_{k+1} = (\bar{u}_1, \ldots, \bar{u}_{k+1}) \in \mathbb{R}^{m\times(k+1)}$, $\bar{V}_k = (\bar{v}_1, \ldots, \bar{v}_k) \in \mathbb{R}^{n\times k}$ and perturbation matrices $E \in \mathbb{R}^{m\times n}$, $\delta b \in \mathbb{R}^{m\times 1}$, such that*

$$\bar{U}_{k+1}(\beta_1 e_1) = b + \delta b, \tag{3.14}$$

$$(Q_A + E)\bar{V}_k = \bar{U}_{k+1}B_k, \tag{3.15}$$

$$(Q_A + E)^T\bar{U}_{k+1} = \bar{V}_k B_k^T + \alpha_{k+1}\bar{v}_{k+1}e_{k+1}^T, \tag{3.16}$$

where

$$\begin{aligned} &\|\bar{U}_{k+1} - U_{k+1}\| \le 2\mu_{k+1} + O(\mu_{k+1}^2), \quad \|\bar{V}_k - V_k\| \le \nu_k + O(\nu_k^2), \\ &\|E\| = O[\|Q_A\|(\tau + \nu_k + \mu_{k+1})], \quad \|\delta b\| = O(\|b\|\epsilon). \end{aligned} \tag{3.17}$$

The full reorthogonalization of u_i and $\tilde{v}_i$ results to that $\mu_{k+1} = O(\epsilon)$ and $\nu_k = O(\epsilon)$. Since $\|Q_A\| \le 1$ and $\epsilon \ll \tau$, we have $\|E\| = O(\tau)$. Therefore, Theorem 3.2 says that the computed B_k is the exact one generated by the Lanczos bidiagonalization process of a slightly perturbed matrix $Q_A + E$ with a slightly perturbed starting vector $b + \delta b$.

4. Accuracy of the regularized solutions. We first gain an insight into the regularization property of the JBD based algorithms. Our following analysis focuses on the pure iterative method, while the hybrid one can be analyzed in a similar way. The following result is appeared in [21].

LEMMA 4.1. *Let x_k^* be the regularized solution generated by the pure iterative method in exact arithmetic. Then*

$$x_k^* = R^{-1}w_k^*, \quad w_k^* = \arg\min_{w\in\mathcal{K}_k(Q_A,b)} \|Q_A w - b\|, \tag{4.1}$$

with

$$\mathcal{K}_k(Q_A, b) = \mathrm{span}\{Q_A^T b, (Q_A^T Q_A)Q_A^T b, \ldots, (Q_A^T Q_A)^{k-1}Q_A^T b\},$$

and the solution subspace

$$\mathcal{R}(Z_k) = R^{-1}\mathcal{K}_k(Q_A, b) = \mathrm{span}\{G(C_A^T C_A)^i C_A^T P_A^T b\}_{i=0}^{k-1}.$$

Since $Q_A = AR^{-1}$, x_k^* is actually the k-th LSQR solution of the preconditioned system $\min_w \|AR^{-1}w - b\|$ with $Rx = w$. We emphasis that the term "preconditioned" is used in a somewhat unconventional way: the "preconditioned" considered here are not aimed at accelerating the convergence of the iterative solver but rather at forcing some specific regularity into the associated solution subspace. In fact, the regularized solution x_k^* has a filtered GSVD expansion and can be explicitly expressed in the generalized right singular vector basis $\{g_i\}_{i=1}^n$ of $\{A, L\}$, which sheds light on the regularization property of the JBD based pure iterative method, for details see [21, Theorem 5.2].

We demonstrate why we can expect that the JBD based algorithms for general form regularization generates a better regularized solution than that of the case $L = I_n$. It is known from [11, Theorem 2.1.1] that c_i decay like the singular values σ_i of A when the matrix $(A^T, L^T)^T$ is well conditioned, and the singular vectors of Q_A have the property that they increase in frequency as the size of the singular values decrease. In the meantime, notice from (2.12) and (2.13) that Q_A and A share the same P_A. Therefore. the problem

$$\min_w \|Q_A w - b\| \tag{4.2}$$

is also ill-posed, which satisfies a similar DPC as problem (1.3). Using the SVD of Q_A in(2.12), the DPC of (4.2) can be written in the following popular simplifying model that is used in [11, 13] and the references therein:

$$|p_{i,A}^T b_{true}| = c_i^{1+\beta}, \quad \beta > 0, \ i = 1, 2, \ldots, n, \tag{4.3}$$

where β is a model parameter that controls the decay rates of $|p_{i,A}^T b_{true}|$. We recall the terminology *effective resolution limit* of (4.2) denoted by η_{res} from Hansen's book [11, Chapter 4, p.71], which means the smallest coefficient $|h_i^T w_{true}|$ that can be recovered from the given Q_A and b, where $H = (h_1, \ldots, h_n)$ is defined in (2.12) and $w_{true} = Q_A^\dagger b_{true}$. It has been shown in [11, Chapter 4] that

$$\eta_{res} = O(\delta^{\frac{\beta}{1+\beta}}), \quad \delta = \|e\|,$$

which implies that the larger the β, i.e. the faster the relative decay of the Fourier coefficients, the smaller the η_{res}, and therefore the more accurately we can compute a regularized solution to (4.2). We mention that a reasonable choice of L will generates a larger β than that of the case $L = I_n$, which can lead to a better regularized w_k^* as well as x_k^* if the solver for solving (4.2) has good enough regularization effects. For the regularization effects of the LSQR for solving (4.2), we recommend readers to refer [17, 18, 19].

We now investigate the accuracy of the computed regularized x_k. Notice that x_k in (2.24) need not to be solved explicitly until the final iteration, so we can assume that (2.24) is solved exactly at each iteration. The solution accuracy of (2.24) at the final step will be analyzed in the end of this section. By Theorem 3.2, the computed $x_k = R^{-1}Q^T\tilde{V}_k y_k = R^{-1}V_k y_k$, where y_k is the solution to

$$\begin{aligned}\min_{y\in\mathbb{R}^k} \|B_k y - \beta_1 e_1\| &= \min_{y\in\mathbb{R}^k} \|\bar{U}_{k+1}B_k y - \bar{U}_{k+1}\beta_1 e_1\| \\ &= \min_{y\in\mathbb{R}^k} \|(Q_A + E)\bar{V}_k y - (b + \delta b)\|.\end{aligned}$$

Let $V_k y_k = w_k$ and $\bar{V}_k y_k = \bar{w}_k$. Notice that Theorem 3.2 implies that $\mathcal{R}(\bar{V}_k) = \mathcal{K}_k(Q_A + E, b + \delta b)$, and $\|R^{-1}\| = \|Z^\dagger\|$ is a moderate quantity. Therefore,

$$\bar{w}_k = \arg \min_{w=\bar{V}_k y} \|(Q_A + E)w - (b + \delta b)\| \tag{4.4}$$

is the k-step LSQR solution to the perturbed problem

$$\min_w \|(Q_A + E)w - (b + \delta b)\|, \tag{4.5}$$

and $\|\bar{w}_k - w_k\| \leq \|\bar{V}_k - V_k\|\|y_k\| = O(\epsilon)$, which implies that $\bar{x}_k = R^{-1}\bar{w}_k$ is approximately $x_k = R^{-1}w_k$ with error $O(\|R^{-1}\|\epsilon)$. Due to the presence of noise e, the regularized solution can never achieve an error in the reconstruction as small as δ, and thus we can use $\bar{x}_k$ and $\bar{w}_k$ instead of x_k and w_k to analyze the accuracy of the regularized solutions.

In order to make the best regularized solution x_{k_1}(the computed version) have the same accuracy as the best regularized solution $x^*_{k_0}$(the exact version), we only need the best regularized solutions of (4.2) and (4.5) have the same accuracy. The problem (4.5) is also ill-posed, because: (i) it can be rewritten in the form

$$(Q_A + E)w = (b_{true} + Ew_{true}) + (e + \delta b - Ew_{true}), \tag{4.6}$$

where $(Q_A + E)w_{true} = (b_{true} + Ew_{true})$ and $(e + \delta b - Ew_{true})$ is the noise; (ii) the components of the backward error term E can be regarded as independent random variables, thus the singular values of $Q_A + E$ decreases monotonically until they tend to settle at the level $O(\tau)$.

We need to give a upper bound of τ, such that the effective resolution limits of (4.2) and (4.6) have the same accuracy. Therefore, problem (4.6) should satisfy the following conditions: **(1)** The noise level in (4.6) is approximately δ, which implies that $\|\delta b - Ew_{true}\| \ll \delta$; **(2)** The DPC of (4.6) has the form

$$|\tilde{p}_i^T(b + \delta b)| \approx \tilde{\sigma}_i^{1+\beta} \tag{4.7}$$

until the noise in $|\tilde{p}_i^T(b + \delta b)|$ dominates, where $\tilde{\sigma}_i$ and $\tilde{p}_i$ are the i-th singular value and left vector of $Q_A + E$; **(3)** if the noise in $|\tilde{p}_i^T(b + \delta b)|$ starts to dominate at $k = k^* + 1$, then $\|E\| \ll c_{k^*}$, i.e., the singular values of $Q_A + E$ are almost not effected by the error term E and thus $\tilde{\sigma}_i \approx c_i$ for $i \leq k^*$.

Condition **(1)** implies that $\tau \ll \delta$ while conditions **(2)** and **(3)** imply that $c_{k^*}^{1+\beta} \approx \tilde{\sigma}_{k^*}^{1+\beta} \approx \delta$ and thus

$$\tau \ll c_{k^*} \approx \delta^{1/(1+\beta)}.$$

In order to make a further investigation of (4.7), we assume specific the decay rate for the singular values dependent on whether the problem is mildly, moderately or severely ill-posed [11]. For problem (4.2), the decay rates of c_i are given by

$$c_i = \begin{cases} \zeta\rho^{-i}, \ \rho > 1 & \text{severely ill-posed;} \\ \zeta i^{-\alpha}, \ \alpha > 1 & \text{moderately ill-posed;} \\ \zeta i^{-\alpha}, \ 1/2 < \alpha \leq 1 & \text{mildly ill-posed.} \end{cases} \tag{4.8}$$

Note that

$$\frac{c_{i+1}}{c_i} = \begin{cases} \rho^{-1} & \text{severely ill-posed;} \\ (\frac{i}{i+1})^\alpha & \text{moderately/mildly ill-posed,} \end{cases}$$

and the distance between the singular values of Q_A become smaller and smaller as their sizes decrease.

By [33, The generlized $\sin\theta$ theorem], we have the perturbation bound

$$|\sin\theta(p_{i,A},\tilde{p}_i)| \le \frac{\|E\|}{c_i - c_{i+1} - \|E\|},$$

where $\theta(p_{i,A},\tilde{p}_i)$ is the angle between two vectors $p_{i,A}$ and $\tilde{p}_i$. Therefore, for $i \le k^*$,

$$\begin{aligned}\|\tilde{p}_i - p_{i,A}\| &= 2|\sin(\theta(p_{i,A},\tilde{p}_i)/2)| \approx |\sin\theta(p_{i,A},\tilde{p}_i)| \\ &\le \frac{\|E\|}{c_i(1-\frac{c_{i+1}}{c_i}) - \|E\|} \approx \frac{\|E\|}{c_i(1-\frac{c_{i+1}}{c_i})}\end{aligned}$$

due to $\|E\| \ll c_i$. Let $\tilde{p}_i = p_{i,A} + \delta p_i$. Since $\tilde{\sigma}_i \approx c_i \gg \tau$ and $c_i^{1+\beta} \ge \delta$ for $i \le k^*$, noticing (4.3), (4.7) implies that

$$|(p_{i,A} + \delta p_i)^T(b + \delta b)| \approx \tilde{\sigma}_i^{1+\beta} \approx c_i^{1+\beta}$$

until the noise in $|\tilde{p}_i^T(b+\delta b)|$ dominates, which can hold if

$$|\delta p_i^T b| \ll c_i^{1+\beta}, \quad i \le k^*, \tag{4.9}$$

due to $|(p_{i,A} + \delta p_i)^T \delta b| = O(\|b\|\epsilon) \ll |\delta p_i^T b|$. (4.9) can be satisfied if

$$\frac{\|E\|\|b\|}{c_i(1-\frac{c_{i+1}}{c_i})} \ll c_i^{1+\beta}, \quad i \le k^*,$$

which results to

$$\|E\| \ll \frac{c_i^{2+\beta}(1-\frac{c_{i+1}}{c_i})}{\|b\|}, \quad i \le k^*.$$

Notice that the minimum of the right term of the above inequality is

$$\frac{c_{k^*}^{2+\beta}(1-\frac{c_{k^*+1}}{c_{k^*}})}{\|b\|} \approx \frac{\delta^{\frac{2+\beta}{1+\beta}}(1-\frac{c_{k^*+1}}{c_{k^*}})}{\|b\|},$$

achieved when $i = k^*$, we conclude the following result.

THEOREM 4.2. *Let JBD(τ) denotes the JBD process with its inner iteration solved by LSQR with tolerance τ as stopping criterion. If*

$$\tau \ll \begin{cases} \frac{\delta^{\frac{2+\beta}{1+\beta}}(1-\rho^{-1})}{\|b\|} & \text{severely ill-posed;} \\ \frac{\delta^{\frac{2+\beta}{1+\beta}}[1-(\frac{k^*}{k^*+1})^\alpha]}{\|b\|} & \text{moderately/mildly ill-posed,} \end{cases} \tag{4.10}$$

then the best regularized solution obtained by the JBD(τ) based pure iterative methods have the same accuracy as that by the JBD based methods in exact arithmetic.

REMARK 4.1. *The assumption (4.8) means that all the singular values of Q_A are simple. However, the matrix Q_A often has multiple singular values, especially when $m > n > p$. The above analysis and results can be extended to the multiple singular*

value case by some modifications of the DPC, and the form of these modifications is mainly due to Jia [19]. Rewrite the SVD of Q_A as

$$Q_A = \widehat{P}_A \begin{pmatrix} \Sigma \\ 0 \end{pmatrix} \widehat{H}^T$$

where $\widehat{P}_A = (\widehat{P}_{1,A}, \ldots, \widehat{P}_{r,A}, \widehat{P}_{\perp,A})$ with $\widehat{P}_{i,A} \in \mathbb{R}^{m\times l_i}$ and $\widehat{H} = (\widehat{H}_1, \ldots, \widehat{H}_r)$ with $\widehat{H}_i \in \mathbb{R}^{n\times l_i}$ are orthogonal, $\Sigma = diag(\widehat{c}_1 I_{l_1}, \ldots, \widehat{c}_r I_{l_r})$ with the r distinct singular values $\widehat{c}_1 > \widehat{c}_2 > \cdots > \widehat{c}_r > 0$, each $\widehat{c}_i$ is l_i multiple and $l_1 + l_2 + \cdots + l_r = n$. The decay rates of $\widehat{c}_i$ can be written in the similar form as (4.8). The DPC corresponding to (4.3) becomes

$$\|\widehat{P}_{i,A}^T b_{true}\| = \widehat{c}_i^{1+\beta}, \quad i = 1, 2, \ldots, r,$$

which states that, on average the Fourier coefficients $\|\widehat{P}_{i,A}^T b_{true}\|$ decay faster than $\widehat{c}_i$.

We write the SVD of $Q_A + E$ in the similar form as that of Q_A(note that the singular values of $Q_A + E$ may not be multiple), such that the left singular vectors can be written as $\widetilde{P} = (\widetilde{P}_1, \ldots, \widetilde{P}_r, \widetilde{P}_\perp)$. By [33, The generlized $\sin\theta$ theorem], we have the perturbation bound of the invariant singular vector spaces

$$\|\sin\Theta(\widehat{P}_{i,A}, \widetilde{P}_i)\| \le \frac{\|E\|}{\widehat{c}_i - \widehat{c}_{i+1} - \|E\|}$$

where $\|\sin\Theta(\widehat{P}_{i,A}, \widetilde{P}_i)\| = \|\widehat{P}_{i,A}\widehat{P}_{i,A}^T - \widetilde{P}_i\widetilde{P}_i^T\|$ is a measure of the 2-norm distance between $\widehat{P}_{i,A}$ and $\widetilde{P}_i$, see [33, 10]. Note that

$$\begin{aligned} |\|\widetilde{P}_i^T b\| - \|\widehat{P}_{i,A}^T b\|| &= |\|\widetilde{P}_i\widetilde{P}_i^T b\| - \|\widehat{P}_{i,A}\widehat{P}_{i,A}^T b\|| \le \|(\widetilde{P}_i\widetilde{P}_i^T - \widehat{P}_{i,A}\widehat{P}_{i,A}^T)b\| \\ &\le \|b\|\|\sin\Theta(\widehat{P}_{i,A}, \widetilde{P}_i)\|, \end{aligned} \tag{4.11}$$

where $|\|\widetilde{P}_i^T b\| - \|\widehat{P}_{i,A}^T b\||$ is the corresponding version of the left term of (4.9). Using the same methods as that analyzing (4.9), (4.10) can be obtained for the multiple singular value case.

In practice, the parameters β, ρ and k^* are hardly to obtain. Fortunately, it is usually the case that $1 - \rho^{-1}$ and $1 - (\frac{k^*}{k^*+1})^\alpha$ are not very small, and $\delta^{\frac{2+\beta}{1+\beta}} < \delta^2$ (the bound can never be achieved for $\beta > 0$). Therefore, if $\|e\|$ or its accurate estimate is known in advance, the solution accuracy τ can be chosen as

$$\tau = \frac{\delta^2}{\|b\|}, \tag{4.12}$$

such that best regularized solutions obtained by the JBD(τ) based pure iterative methods have the same accuracy as that obtained by the JBD based methods in exact arithmetic. Numerical examples will show that the solution accuracy τ in (4.12) is always enough, and for many problems, (4.12) can even be relaxed by choosing $\tau = \delta^{1+\gamma}/\|b\|$ for some $0 < \gamma < 1$. For most applications where the noise level $\varepsilon = \|e\|/\|b\|$ is not very small ($\varepsilon \ge 10^{-3}$), it is enough to solve (2.11) by the MATLAB function lsqr.m with the default stopping tolerance 10^{-6}.

Finally we investigate the solution accuracy of (2.24) at the final iteration in order to obtain the desired regularized solution x_k. Suppose the best regularized solutions

generated by JBD in exact arithmetic and JBD(τ) are obtained at iteration k_0 and k_1 respectively, then we need to solve the following two problems:

$$\begin{pmatrix} A \\ L \end{pmatrix} x = \widetilde{V}_{k_0}^* y_{k_0}^*, \tag{4.13}$$

$$\begin{pmatrix} A \\ L \end{pmatrix} x = \widetilde{V}_{k_1} y_{k_1} \tag{4.14}$$

and x_{k_0} is the solution to (4.13). Suppose that (4.14) is solved by using the LSQR with tolerance ρ as stopping criterion, then the computed x_{k_1} is the exact solution of

$$\arg\min_{x\in\mathbb{R}^n} \|(Z+K)x - \widetilde{V}_{k_1} y_{k_1}\| \tag{4.15}$$

where

$$K = -\frac{r^T r Z}{\|r\|^2}, \quad r = \widetilde{V}_{k_1} y_{k_1} - Z x_{k_1}$$

satisfying

$$\frac{\|K\|}{\|Z\|} = \frac{\|Z^T r\|}{\|Z\|\|r\|} \le \rho.$$

Notice that

$$\begin{aligned} \widetilde{V}_{k_0}^* y_{k_0}^* - \widetilde{V}_{k_1} y_{k_1} &= Q V_{k_0}^* y_{k_0}^* - Q\bar{V}_{k_1} y_{k_1} + Q(\bar{V}_{k_1} - V_{k_1}) y_{k_1} + (Q V_{k_1} - \widetilde{V}_{k_1}) y_{k_1} \\ &= Q(w_{k_0}^* - w_{k_1}) + Q(\bar{V}_{k_1} - V_{k_1}) y_{k_1} + (Q V_{k_1} - \widetilde{V}_{k_1}) y_{k_1}, \end{aligned}$$

and $\|\bar{V}_{k_1} - V_{k_1}\| = O(\epsilon)$, $\|Q V_{k_1} - \widetilde{V}_{k_1}\| = O(\tau)$, see (3.8), (3.13) and (3.17). Assume that $\|w_{k_0}^* - w_{true}\| = O(\delta^\sigma)$ where $0 < \sigma < 1$. Since $w_{k_1}^*$ and w_{k_1} are of same accuracy as regularized approximations to w_{true}, it follows that $\|w_{k_0}^* - w_{k_1}\| \ll \|w_{k_0}^* - w_{true}\|$ and thus

$$\frac{\|\widetilde{V}_{k_0}^* y_{k_0}^* - \widetilde{V}_{k_1} y_{k_1}\|}{\|\widetilde{V}_{k_0}^* y_{k_0}^*\|} \le C_1 \delta^\sigma,$$

where C_1 is a moderate constant. Notice that (4.15) is the perturbation problem of the consistent system (4.13), by [15, Theorem 20.1], we have

$$\|x_{k_0}^* - x_{k_1}\| \le \frac{2\kappa(Z)\|x_{k_0}^*\|\xi}{1 - \kappa(Z)\xi}, \quad \xi = \max(\rho, C_1\delta^\sigma). \tag{4.16}$$

Since

$$\|x_{true} - x_{k_1}^*\| = \|R^{-1}(w_{true} - w_{k_1}^*) \le \|Z^\dagger\|\|w_{true} - w_{k_0}^*\| = O(\|Z^\dagger\|\delta^\sigma),$$

in order to make the computed x_{k1} has the same regularized accuracy as x_{k0}^*, from (4.16), we only need to choose $\rho \ll C_1\delta^\sigma$. Since $\delta^\sigma > \delta$, in practice it is enough to choose $\rho = \delta$.

REMARK 4.2. *For the JBD based hybrid method, the solution subspace of x_k^λ is the same as that of x_k [24], and Tikhonov regularization is used to the projected problem of $\min_w \|Q_A w - b\|$. Therefore, the above analysis and results of the pure iterative method still hold for the hybrid method.*

5. Some implementation details. In this section, we discuss some implementation details of the two JBD based regularization algorithms, including some methods for choosing regularization parameters or terminating iterations at the appropriate step and efficient methods to update solutions step by step. Here we discuss the algorithms in exact arithmetic and we still use the notations appeared in Section 2 to denote the quantities obtained in exact arithmetic.

For the hybrid method, rather than determining μ_k^{opt} for each projected problem (2.20), Kilmer *et al.* [24] use the L-curve criterion to tentatively estimate λ^{opt}. They assume that a set of λ-values is prescribed, then for each k an L-curve can be determined by drawing the picture of $(\log\|Ax_k^\lambda - b\|, \log\|Lx_k^\lambda\|)$ for the given set of λ-values and the value of the parameter on the "corner" can then be computed. For sufficiently large k where the dominant GSVD components of $\{A, L\}$ have been captured, the λ-value at the corner should stagnate, and we pick up the λ-value at the corner as an approximate λ^{opt}. However, this approach seems not efficient and robust, since it is usually difficult to choose a good a-prior set of λ-values which includes the optimal regularization parameter λ^{opt} or its good approximation. In [21] the authors suggested using the GCV or WGCV method to estimate the optimal μ_k^{opt} at each iteration. These two methods often suffer from over- or under-estimate regularization parameters of the projected problem, and in some cases the estimated μ_k^{opt} does not converge to the global optimal regularization parameter λ^{opt} [4, 31]. As a consequence, the regularized solutions may exhibit semi-convergence behavior for k sufficiently large, and it may be hard to terminate the hybrid algorithm properly, and We mention that determining μ_k^{opt} for each (2.20) by the GCV or WGCV method needs to compute the GSVD of $\{B_k, \bar{B}_k\}$ at cost of $O(k^3)$ flops.

Here we propose an automatic parameter updating method, called "secant update", to update estimated regularization parameters step by step, in order to approximate λ^{opt}. The method was first proposed to find optimal regularization parameters for the Arnoldi-Tikhonov hybrid methods [9]. We show that this method can be adapted to find approximate λ^{opt} for the JBD based hybrid method, which is efficient and robust. Assume we know $\delta = \|e\|$ or its accurate estimate. Then a successful strategy to determine a suitable regularization parameter is the discrepancy principle. At each iteration we define the function

$$\varphi_k(\lambda) = \|b - Ax_k^\lambda\| = \|\beta_1 e_1 - B_k y_k^\lambda\|,$$

and we say that the discrepancy principle is satisfied as soon as $\varphi_k(\lambda) \leq \eta\delta$ where $\eta \gtrapprox 1$. In order to obtain appropriate k and λ, we consider solving the nonlinear equation

$$\varphi_k(\lambda) = \eta\delta, \tag{5.1}$$

such that suitable values for λ and k can be determined simultaneously. Suppose that at step k, we use the parameter λ_{k-1} which is obtained in the previous step (λ_0 must be set to an initial value by the user). Notice that $\varphi_k(\lambda)$ is monotonically increasing and can be approximated by the linear function

$$f(\lambda) = \varphi_k(0) + \frac{\varphi_k(\lambda_{k-1}) - \varphi_k(0)}{\lambda_{k-1}}\lambda, \tag{5.2}$$

which interpolates $\varphi_k(\lambda)$ at 0 and λ_{k-1}. To select λ_k for the next step we impose $\varphi_k(\lambda_k) \approx \eta\delta$, and use the approximation $\varphi_k(\lambda) \approx f(\lambda)$ to solve the equation

$$f(\lambda_k) = \eta\delta,$$

which yields

$$\lambda_k = \frac{\eta\delta - \varphi_k(0)}{\varphi_k(\lambda_{k-1}) - \varphi_k(0)}\lambda_{k-1}. \tag{5.3}$$

A geometric interpretation of finding λ_k is displayed in Fig.1. Note that $\varphi_k(0) =$

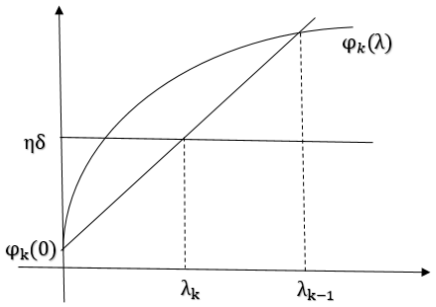

FIG. 1. *Zero finder by secant method*

$\|b - Ax_k\|$ is the residual norm of the k-th solution of the JBD based pure iterative method, which can be updated recursively from $\varphi_{k-1}(0)$ without forming x_k explicitly. We will discuss this for the pure iterative method in detail later. For small values of k instability of (5.3) may occur due to that we may have $\varphi_k(0) > \eta\delta$. In this occasion the result of (5.3) may be negative and we use

$$\lambda_k = \Big|\frac{\eta\delta - \varphi_k(0)}{\varphi_k(\lambda_{k-1}) - \varphi_k(0)}\Big|\lambda_{k-1} \tag{5.4}$$

to guarantee the positive of λ_k. In practice, we choose $\eta > 1$ slightly, e.g. $\eta = 1.01$ or smaller, and we use the default value $\lambda_0 = 1.0$. We find that numerically (5.4) is very stable in the sense that after the discrepancy principle is satisfied, λ_k is almost constant and $\varphi_k(\lambda_{k-1})$ stagnates.

For the pure iterative method, from Lemma 4.1 we know that the optimal iteration k_0 of (2.21) is the same as that of (4.2). Notice that

$$\|Ax_k - b\| = \|B_k e_1 - \beta_1 e_1\| = \|Q_A w_k - b\|.$$

Using the discrepancy principle, we stop the algorithm at the first iteration k satisfying

$$\|Q_A w_k - b\| = \|B_k y_k - \beta_1 e_1\| \le \eta\delta \tag{5.5}$$

with $\eta > 1$ slightly if $\|e\|$ or its accurate estimate is known in advance. We then use such k as an estimate of the optimal iteration k_0. Another approach to estimate k_0 is the L-curve method, which does not need $\|e\|$ a prior. For the problem (4.2), since the residual norm $\|Q_A w_k - b\| = \|B_k y_k - \beta_1 e_1\|$ monotonically decreases and $\|w_k\| = \|y_k\|$ monotonically increases with respect to k, we can plot the curve

$$(\log \|B_k y_k - \beta_1 e_1\|, \log \|y_k\|) \tag{5.6}$$

and then determine k at its overall corner as an estimate of k_0. The L-curve method of form (5.6) often suffers severely from over-estimate k_0 and thus the solution is under-regularized, especially for problems with small noise levels [11]. In practice,

fortunately, we find that the semi-norm $\|Lx_k\| = \|\bar{B}_k y_k\|$ monotonically increases with respect to k (although in theory, $\|Lx_k\|$ is not monotonically increasing for all problems), we can use the L-curve

$$\left(\log \|B_k y_k - \beta_1 e_1\|, \log \|\bar{B}_k y_k\|\right) \tag{5.7}$$

to estimate k_0. We find that numerically, the k at the corner of the curve (5.7) is usually slightly smaller than k_0, and the accuracy of x_k is not far from that of x_{k_0}.

We finally show how to compute $\varphi_k(0) = \|B_k y_k - \beta_1 e_1\|$, $\|y_k\|$ and $\|\bar{B}_k y_k\|$ efficiently. Since w_k is the k-th LSQR solution of (4.2), the method of updating w_k can be adapted to update $z_k = \widetilde{V}_k y_k = QV_k y_k = Qw_k$. Following [30, Algorithm LSQR], we summarize the algorithm of updating z_k.

Algorithm 2 Updating procedure

Let $z_0 = 0_{m+p},\ q_1 = \tilde{v}_1,\ \bar{\phi}_1 = \beta_1,\ \bar{\rho}_1 = \alpha_1$
for $i = 1, 2, \ldots, k$, **do**
  $\rho_i = (\bar{\rho}_i^2 + \beta_{i+1}^2)^{1/2}$
  $\bar{c}_i = \bar{\rho}_i/\rho_i,\ \bar{s}_i = \beta_{i+1}/\rho_i$
  $\theta_{i+1} = \bar{s}_i \alpha_{i+1},\ \bar{\rho}_{i+1} = -\bar{c}_i \alpha_{i+1}$
  $\phi_i = \bar{c}_i \bar{\phi}_i,\ \bar{\phi}_{i+1} = \bar{s}_i \bar{\phi}_i$
  $z_i = z_{i-1} + (\phi_i/\rho_i) q_i$
  $q_{i+1} = \tilde{v}_{i+1} - (\theta_{i+1}/\rho_i) q_i$
end for

It has been proved in [30] that

$$\varphi_k(0) = \|B_k y_k - \beta_1 e_1\| = \bar{\phi}_{k+1}. \tag{5.8}$$

Since

$$z_k = \tilde{V}_k y_k = \begin{pmatrix} Q_A \\ Q_L \end{pmatrix} w_k = \begin{pmatrix} Q_A w_k \\ Q_L w_k \end{pmatrix}, \quad Q_L w_k = Q_L R R^{-1} w_k = L x_k,$$

it follows that

$$\|y_k\| = \|z_k\|, \qquad \|Lx_k\| = \|\bar{B}_k y_k\| = \|z_k(m+1 : m+p)\|. \tag{5.9}$$

Therefore, $\|B_k y_k - \beta_1 e_1\|$, $\|y_k\|$ and $\|\bar{B}_k y_k\|$ can be computed by Algorithm 2 efficiently. We mention that we only need to compute x_k by solving (2.24) at the final iteration, where $\widetilde{V}_k y_k = z_k$ can be updated efficiently by Algorithm 2 .

6. Numerical examples. In this section, we present some numerical experiments to investigate the performance of the two JBD based regularization algorithms. We illustrate some results in Section 3, which describe the numerical behavior of the joint bidiagonalization. We show how the solution accuracy of (2.11) influences the accuracy of the regularized solutions and demonstrate the choice of τ in (4.12). We denote the hybrid methods using WGCV and secant update as parameter-choice methods by JBD-WGCV and JBD-sec respectively, and the pure iterative method is abbreviated as JBDQR following [21]. We compare accuracy of the regularized solutions obtained by the JBD based hybrid method and pure iterative method by using the relative reconstruction error

$$RE(k) = \frac{\|x_k^{reg} - x_{true}\|}{\|x_{true}\|} \quad or \quad RE_L(k) = \frac{\|L(x_k^{reg} - x_{true})\|}{\|Lx_{true}\|} \tag{6.1}$$

to plot the convergence curve of each algorithm with respect to k, where x_k^{reg} denotes the regularized solutions obtained by each of the algorithms. We also use two 2D image deblurring problems to test the JBD based regularization algorithms for restoring blurred and noisy images.

We choose some one dimensional examples from the regularization toolbox [12], and two 2D image deblurring problems where the blurs PRblurspeckle and PRblurgauss are from [8] and the two images are "satellite" and "Grain" from [1]. All test problems are described in Table 1.

All the computations are carried out in MATLAB R2017b on Intel(R) Core(TM) i7-5500U CPU 2.40GHz processor and 4 GB RAM with the machine precision $\epsilon = 2.22 \times 10^{-16}$ under the Miscrosoft Windows 10 64-bit system. Some codes in the software packages of [12, 1, 8] are used and adapted for our numerical experiments.

TABLE 1
The description of test problems

Problem	Description	Ill-posedness	$m \times n$
shaw	1D image restoration model	severe	1024×1024
gravity	1D gravity surveying problem	servere	1024×1024
heat	Inverse heat equation	moderate	2048×2048
deriv2	Computation of second derivative	moderate	2048×2048
PRblurspeckle	2D image deblurring,"satellite"	moderate	16384×16384
PRblurgauss	2D image deblurring, "Grain"	mild	65536×65536

6.1. One dimensional case. For one dimensional problems shaw, gravity, heat and deriv2, we use the codes of [12] to generate A, x_{true} and $b_{true} = Ax_{true}$. We mention that deriv2 has three kinds of right-hand sides, distinguished by the parameter "$case = 1, 2, 3$" and we use the default "$case = 1$". We add a white noise e with zero mean and a prescribed noise level

$$\varepsilon = \frac{\|e\|}{\|b_{true}\|}$$

to b_{true} and form the noisy $b = b_{true} + e$. Since x_{true} is known, we can compute the optimal regularization parameter μ_k^{opt} in (2.20) at each iteration for the hybrid method, by setting

$$y_k^{true} = \widetilde{V}_k^T \begin{pmatrix} A \\ L \end{pmatrix} x_{true},$$

to be the true solution of the k-th projected problem. The hybrid method with μ_k^{opt} at each iteration is denoted by JBDhyb-opt and we would compare convergence curves and regularized parameters of JBD-WGCV, JBD-sec with that of JBD-opt. We choose

$$L = L_1 = \begin{pmatrix} 1 & -1 & & & \\ & 1 & -1 & & \\ & & \ddots & \ddots & \\ & & & 1 & -1 \end{pmatrix} \in \mathbb{R}^{(n-1)\times n}, \tag{6.2}$$

which is a scaled discrete approximation of the first derivative operator in one dimensional case, as regularization matrix. We mention that for the scaled discrete approximation of the second derivative operator, we have observed very similar phenomena and we only report the results on $L = L_1$.

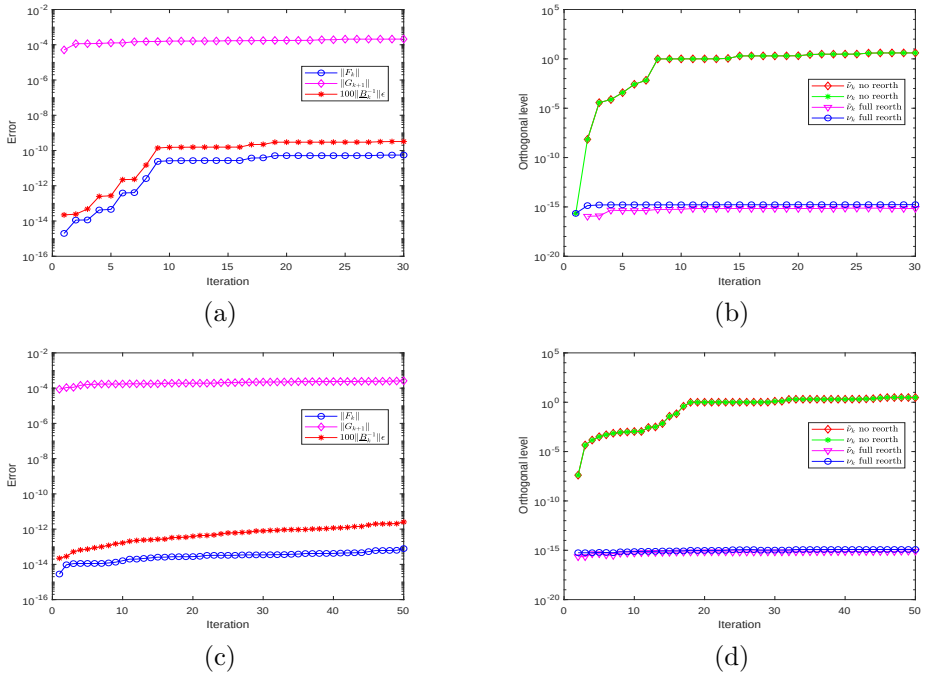

FIG. 2. *Errors in* (3.10), (3.11) *and orthogonal levels of* $\widetilde{V}_k$, V_k, $\varepsilon = 10^{-4}$, $\tau = 10^{-6}$*: (a)* shaw, $\|F_k\|$ *with bound* $100\|\underline{B}_k^{-1}\|\epsilon$ *and* $\|G_{k+1}\|$*; (b)* shaw*, orthogonal levels of* $\widetilde{V}_k$, V_k *with no and full reorthogonalization; (c)* heat, $\|F_k\|$ *with bound* $100\|\underline{B}_k^{-1}\|\epsilon$ *and* $\|G_{k+1}\|$*; (d)* heat*, orthogonal levels of* $\widetilde{V}_k$, V_k *with no and full reorthogonalization.*

First we demonstrate the result of Theorem 3.1. We choose the severely ill-posed problem shaw and moderately ill-posed problem heat to implement the JBD process respectively. For both two problems the noise level is $\varepsilon = 10^{-4}$ and the stopping tolerance of lsqr.m for solving (2.11) are set to be $\tau = 10^{-6}$. From figure 2, we find that for shaw, the computed errors appeared in (3.10) and (3.11) are consistent with our theoretical results: $\|F_k\|$ gradually increases with bound $O(\|\underline{B}_k^{-1}\|\epsilon)$ while $\|G_{k+1}\|$ remains almost constant and $\|G_{k+1}\| \approx 10^{-4} = O(\tau)$. With no reorthogonalization, the orthogonality of $\widetilde{V}_k$ and V_k quickly lost, while the orthogonal levels of both $\widetilde{V}_k$ and V_k remain $O(\epsilon)$ if full reorthogonalization is used. For heat we can get the same results from figure 2. Besides, we find that our assumption (3.13) is very reasonable for ill-posed problems shaw and heat, since k is usually not too big and $\|\underline{B}_k^{-1}\|\epsilon \ll \tau$ before we terminate the iterations of the JBD based regularized methods. The result of Theorem 3.2, which contains backward error terms, cannot be directly validated by numerical experiments, but the numerical results shown in figure 2 ulteriorly confirm it.

In order to illustrate how the accuracy of the regularized solutions be influenced by the solution accuracy of the inner least squares problem (2.11), the tolerance τ as stopping criterion of lsqr.m for solving (2.11) are set to be four values $\tau = \delta^3/\|b\|$, $\delta^2/\|b\|$, $\delta^{1.5}/\|b\|$, $\delta/\|b\|$ respectively. We compute the relative errors $RE(k)$ for JBDQR corresponding the four τ at each iteration, where x_k are computed by solving (2.24) with tolerance 10^{-10} as stopping criterion at each iteration. The semi-convergence curves of the test problems corresponding to the four different τ are shown

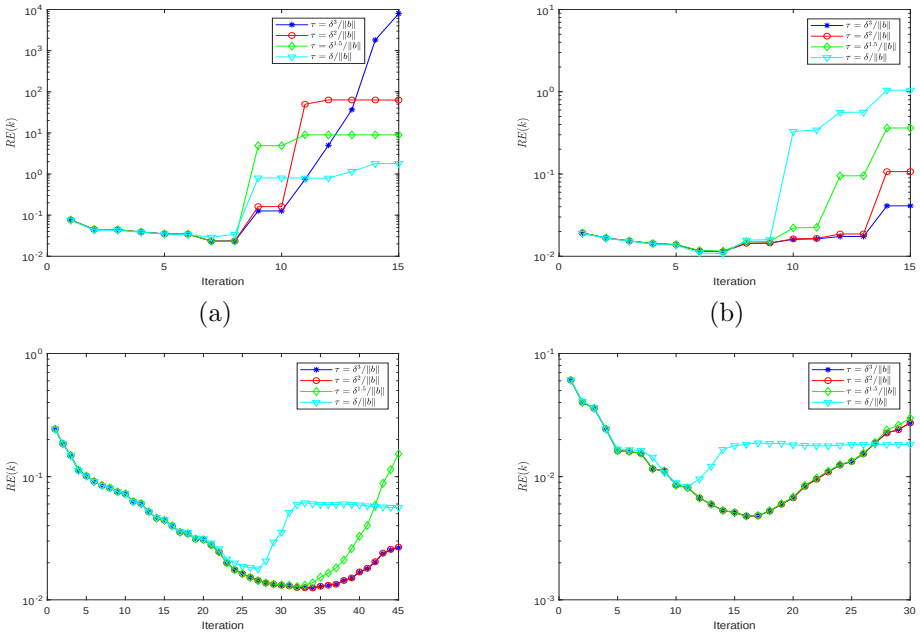

FIG. 3. *Comparison of accuracy of regularized solutions obtained by* JBDQR *with different choices of* τ, $\varepsilon = 10^{-4}$*: (a)* shaw*; (b)* gravity*; (c)* heat*; (d)* deriv2.

in figure 3. We find that the relative errors have the same accuracy for $\tau = \delta^3/\|b\|$ and $\tau = \delta^2/\|b\|$ until semi-convergence appears (at k_0), and this is even true for a few steps $k > k_0$ for the two moderate ill-posed problems heat and deriv2 and the severe ill-posed problem gravity. For $\tau = \delta^{1.5}/\|b\|$, the accuracy of regularized solutions are the same as that of $\delta^2/\|b\|$ for the test problem except heat (which is only slightly poor) until semi-convergence appears, while for $\tau = \delta\|b\|$, the semi-convergence appears earlier than that of $\delta^2/\|b\|$ and the accuracy of the optimal solutions are less than that of $\delta^2/\|b\|$ except for gravity. Therefore, the solution accuracy $\tau = \delta^2/\|b\|$ given in (4.12) is enough to obtain regularized solutions with ideal optimal accuracy, and for some problems, the τ can be relaxed by choosing $\tau = \delta^{1+\gamma}/\|b\|$ for some γ slightly smaller than 1. Through the rest of our numerical experiments, we choose $\tau = \delta^2/\|b\|$, and use the default stopping tolerance 10^{-6} in lsqr.m to solve (2.24) when we need to compute x_k or x_k^λ.

TABLE 2
Relative errors $RE_L(k)$ *and estimated* k_0 *for* JBDQR, $\varepsilon = 10^{-3}$.

Methods	shaw	gravity	heat	deriv2
optimal	0.2845 (6)	0.2803 (5)	0.1529 (25)	0.2533 (10)
L-curve (5.6)	5.9620e+03 (14)	487.6068 (18)	0.6842 (36)	8.0219 (22)
L-curve (5.7)	0.3020 (3)	0.2810 (2)	0.1648 (22)	0.3521 (4)
DP	0.3030 (2)	0.2821 (1)	0.1566 (23)	0.2668 (8)

To illustrate the methods for estimating optimal stopping iteration k_0 for JBDQR, we plot the relative errors $RE_L(k)$ of the iterations for the four test problems, and

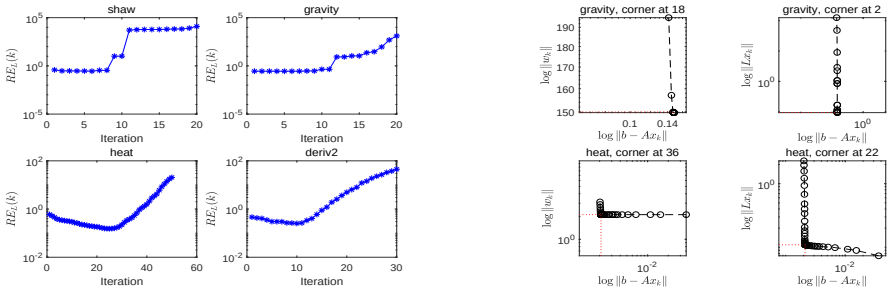

(a) (b)

FIG. 4. *Relative errors $RE_L(k)$ of* JBDQR *and L-curve of forms* (5.6) *and* (5.7), $\varepsilon = 10^{-3}$*: (a) relative error plots of the four test problems; (b) L-curve of* gravity *and* heat.

we draw the L-curve of forms (5.6) and (5.7) for problem gravity and heat. From figure 4, we find that $RE_L(k)$ also exhibit typical semi-convergence behavior for all the test problems. For the moderate ill-posed problem heat, the L-curve of the two forms have better "L" shape than that of the severely ill-posed problem gravity, which due to that for severely ill-posed problems JBDQR often converges very fast and uses very few iterations to achieve the semi-convergence point. In table 2, we display the relative errors $RE_L(k)$ and the corresponding stopping iterations estimated by the L-curve of the two forms and the discrepancy principle (DP) by setting $\eta = 1.001$ (since the noise level is known). For comparison, we also display the optimal relative errors at k_0. As we can see from the table, for the test problems, the L-curve of the form (5.6) suffers severely from over-estimating the true k_0, resulting to under-regularized solutions with poor accuracy, while the L-curve of form (5.7) usually under-estimates the true k_0 slightly and accuracy of the corresponding over-regularized regularized solutions are not too poor, within the acceptable range. In the rest of our numerical experiments, we choose L-curve of the form (5.7) to estimate k_0. The discrepancy principle always under-estimates the true k_0 for the test problems. We mention that the choice of η is critical for estimating k_0, and usually the more bigger η, the estimated k_0 is more under-estimated.

TABLE 3
Relative errors $RE(k)$ and stopping iterations, $\varepsilon = 10^{-3}$.

Methods	shaw	gravity	heat	deriv2
JBDQR(optimal)	0.0540 (6)	0.0320 (8)	0.0199 (25)	0.0149 (10)
JBDQR(L-curve)	0.0703 (2)	0.0321 (2)	0.0227 (23)	0.0267 (4)
JBDQR(DP)	0.0703 (2)	0.0323 (1)	0.0293 (21)	0.0184 (6)
JBDhyb-opt	0.0687 (8)	0.0322 (3)	0.0217 (31)	0.0160 (13)
JBD-WGCV	0.1056 (4)	0.0339 (3)	0.0709 (14)	0.0403 (5)
JBD-sec	0.0749 (11)	0.0322 (7)	0.0258 (42)	0.0197 (18)

Figure 5 depicts the convergence behavior of JBDQR and the JBD based hybrid methods including JBDhyb-opt, JBD-WGCV and JBD-sec. In the convergence curves, we mark the points corresponding to optimal k_0 for JBDQR and stopping iterations for JBD-WGCV and JBD-sec. The relative errors $RE(k)$ and the corresponding stopping iterations are listed in table 3, where for JBDhyb-opt we choose the first stabilized values appeared in the convergence curve. Meanwhile, we plot the regularization

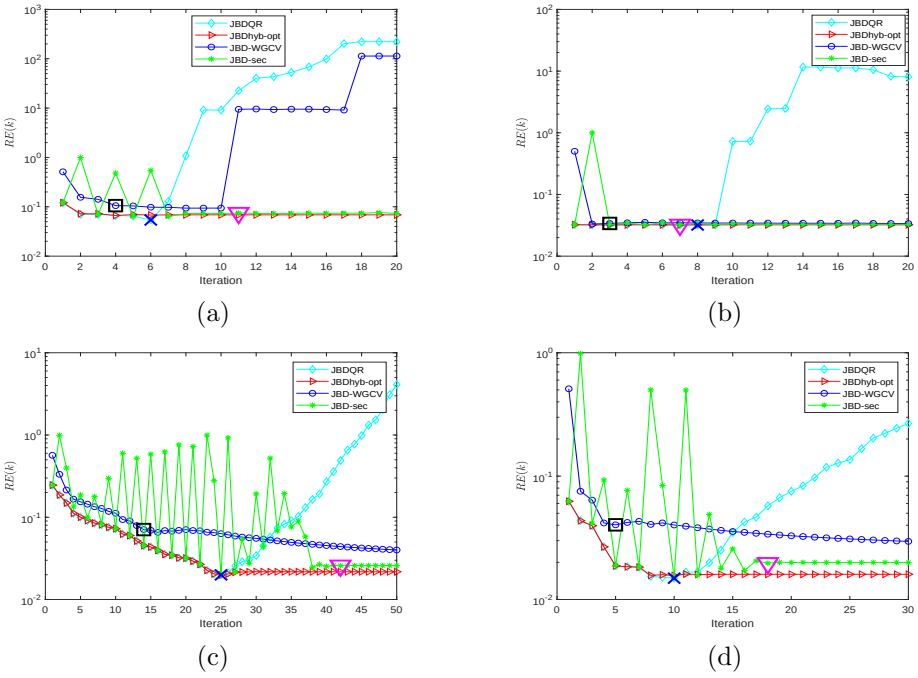

FIG. 5. *Relative error plots of the four test problems,* $\varepsilon = 10^{-3}$*: (a)* shaw*; (b)* gravity*; (c)* heat*; (d)* deriv2.

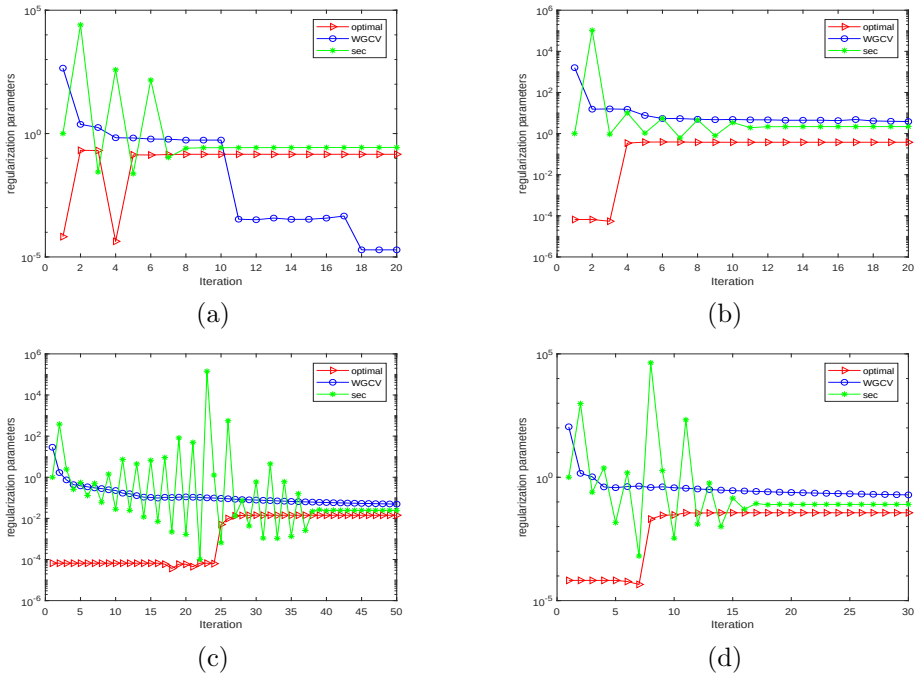

FIG. 6. *Comparison of regularized parameters for the JBD-based hybrid methods,* $\varepsilon = 10^{-3}$*: (a)* shaw*; (b)* gravity*; (c)* heat*; (d)* deriv2.

parameters of hybrid methods at each iteration in figure 6. In some cases, the convergence behavior of the JBD-WGCV is not stable. For shaw, it under-estimates μ_k^{opt} for large k, resulting in semi-convergence behavior, which was also shown in [4] for the Lanczos-hybrid method. Let $G(\omega_k, \mu_k)$ be the WGCV function at step k with ω_k as the adapted weight parameter. In this case the values of $G(\omega_k, \mu_k)$ will still converge to a fixed value. Therefore, following [4], we choose to terminate the iterations when these values change very little, by using

$$\left|\frac{G(\omega_{k+1}, \mu_{k+1}) - G(\omega_k, \mu_k)}{G(\omega_1, \mu_1)}\right| < tol1 \tag{6.3}$$

as the stopping criterion, and we choose $tol1 = 10^{-6}$ here. For JBD-sec we use $\eta = 1.001$ in (5.4), and the convergence curves oscillate for small values of k, due to the fact that $\varphi_k(0) > \eta\delta$. As k becomes bigger, the secant-update approach exhibits a very stable progress since the norm of the discrepancy $\varphi_k(\lambda_{k-1})$ stagnates and the values of the regularized parameters λ_k remains almost constant. To terminate the iteration, we choose $k+s_0$ as the stopping iteration, where k is the first step satisfying

$$\varphi_k(0) \le \eta\delta, \quad and \left|\frac{\varphi_i(\lambda_{i-1}) - \eta\delta}{\eta\delta}\right| \le tol2, \quad i = k, \ldots, k+s_0, \tag{6.4}$$

and we set $s_0 = 4$ and $tol2 = 0.1$ here.

We observe from the figures 5, 6 and table 3 that, the optimal regularized solution x_{k_0} of JBDQR is the best among these algorithms, of which the accuracy is slightly better than that of the convergent solution of JBDhyb-opt (these two solutions cannot be obtained in practice since x_{true} is unknown). The discrepancy principle and the L-curve of form (5.7) under-estimate the optimal k_0 for the test problems, resulting over-regularized solutions, of which the accuracy are within the acceptable range. The regularized solutions of JBD-WGCV are usually less accurate than that of JBDhyb-opt, and converge slowly to the solutions of JBDhyb-opt for heat and deriv2. Comparing with JBD-WGCV, the convergence curves of JBD-sec are more close to that of JBDhyb-opt, due to that the regularized parameters of JBDhyb-opt are more close to the optimal ones obtained by JBDhyb-opt. Therefore, regularized solutions of JBD-sec are more accurate than that of JBD-WGCV, and the convergence behaviors are more efficient and stable.

To show the regularization ability of the JBD based methods, we also use the standard LSQR methods to regularize problems shaw and deriv2. We draw the curves of x_{true} and the regularized solutions obtained by LSQR and JBDQR at the optimal steps in figure 7. For shaw, the reconstructed solution obtained by JBDQR is similar as that by LSQR, while for deriv2, the optimal reconstructed solution obtained by LSQR suffers severely from oscillation, much poor than that by JBDQR.

6.2. Two dimensional case. We test 2D image deblurring problems listed in Table 1 with the goal to restore an image x_{true} from a blurred and noisy image $b = b_{true} + e$. For the background of image deblurring, we recommend readers to refer [14, 1, 27]. For PRblurspeckle, which simulates spatially invariant blurring caused by atmospheric turbulence, we use the true image "satellite" with image size of $N = 128$(i.e., the true and blurred images have 128×128 pixels), while the boundary condition is zero and the level of blurring is set to be moderate. For PRblurgauss, which simulates a spatially invariant Gaussian blur, we use the true image "Grain" with image size of $N = 256$, the default boundary condition (reflective), and a mild level blurring. We add 1% Gaussian noise(i.e., the noise level $\varepsilon = 0.01$) to b_{true} in

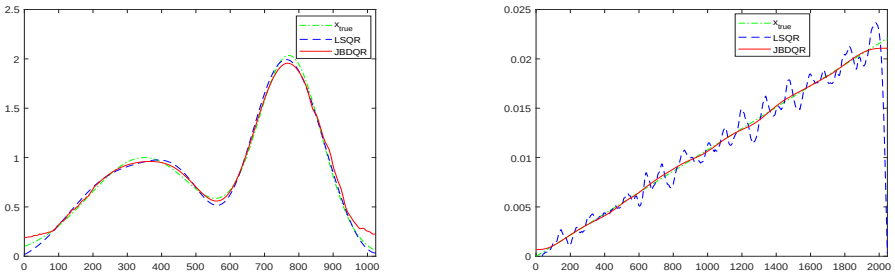

(a) (b)

FIG. 7. *Comparison of reconstructed solutions obtained by* LSQR(optimal) *and* JBDQR(optimal), $\varepsilon = 10^{-3}$*: (a)* shaw*; (b)* deriv2*.*

the two problems. Specifically, we generate the data using the MATLAB codes in [8], e.g.,

```
[A, b_true, x_true, ProbInfo] = PRblurspeckle(options);
[b, NoiseInfo] = PRnoise(b_true, 'gauss', NoiseLevel).
```

For the two problems, A is a `psfMatrix` object that overloads various standard MATLAB operations. Figure 8 shows the resulting true images x_{true} (left) and the blurred and noisy images b (right).

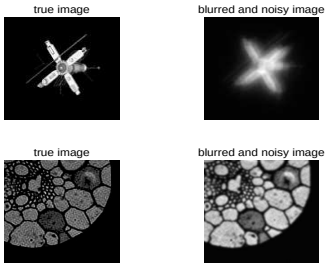

FIG. 8. *Image deblurring test data:* top *true and blurred and noisy images of "satellite";* bottom *true and blurred and noisy images of "Grain".*

For the JBD based algorithms, we choose the regularization matrix

$$L = \begin{pmatrix} I_N \otimes L_1 \\ L_1 \otimes I_N \end{pmatrix} \in \mathbb{R}^{N(N-1)\times N^2} \tag{6.5}$$

with L_1 defined in (6.2) and I_N the identity matrix of order N. Following (4.12), the solution accuracy of (2.11) is set as $\tau = \delta^2/\|b\|$. We use the L-curve of the form (5.7) and the discrepancy principle with $\eta = 1.001$ for estimating the optimal k_0. For JBD-sec we also choose $\eta = 1.001$ in (5.4). The parameters used for terminating JBD-WGCV are set to be $tol1 = 10^{-8}$ in (6.3) and for terminating JBD-sec are set to be $tol2 = 0.1$ and $s_0 = 9$ in (6.4). For the aim of comparison, we also use the standard LSQR method to restored the test images.

Figure 9 depicts relative errors $RE(k)$ of these regularized methods at each iteration, and the restored images at the optimal or stopping iterations. We also mark the points corresponding to optimal iterations for JBDQR and LSQR and stopping

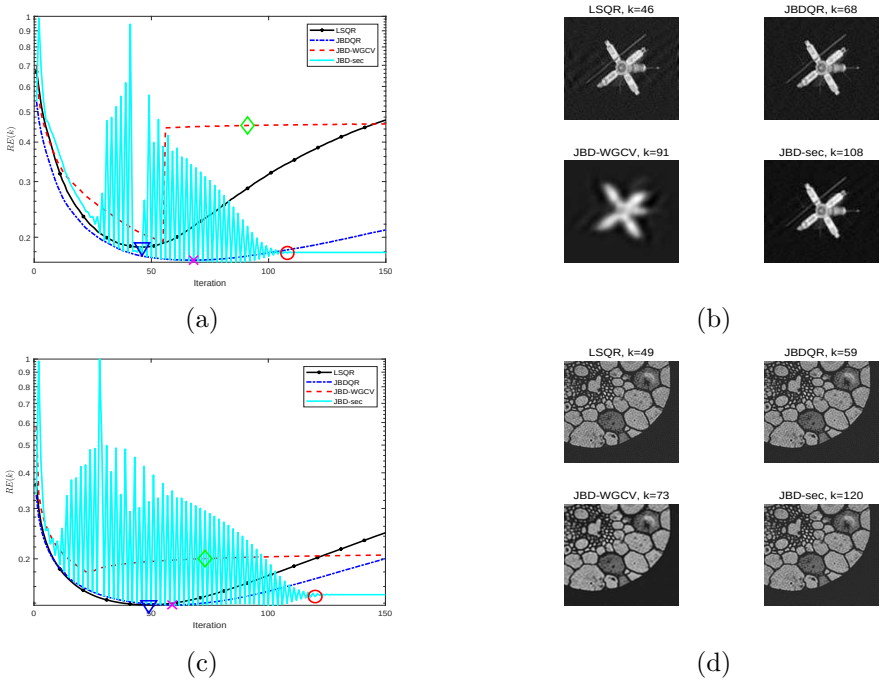

FIG. 9. *Results of the image deblurring test problems, $\varepsilon = 0.01$: (a) relative error plots of* PRblurspeckle*; (b) restored images of "satellite"; (c) relative error plot of* PRblurgauss*; (d)restored images of "Grain".*

TABLE 4
Relative errors $RE(k)$ and stopping iterations, $\varepsilon = 0.01$

Methods	PRblurspeckle	PRblurgauss
LSQR(optimal)	0.1861 (46)	0.1380 (49)
JBDQR(optimal)	0.1693 (68)	0.1381 (59)
JBDQR(DP)	0.1793 (40)	0.1521 (26)
JBDQR(L-curve)	0.1694 (71)	0.1424 (39)
JBD-WGCV	0.4515 (91)	0.2003 (73)
JBD-sec	0.1784 (108)	0.1476 (120)

iterations for JBD-WGCV and JBD-sec. The relative errors at the optimal or stopping iterations are listed in table 4. For PRblurspeckle, the accuracy of the optimal x_{k_0} obtained by JBDQR is obviously higher than that by LSQR. The convergence curve of JBD-sec first oscillates, then gradually converges as k becomes bigger and stagnates almost constant, and the convergent solution is better than the optimal one obtained by LSQR. For JBD-WGCV, the convergence curve exhibits semi-convergence behavior, and the stopping criterion is not robust for problem PRblurspeckle, resulting a poor restored image. For PRblurgauss, the optimal x_{k_0} by JBDQR has the same accuracy as that by LSQR, which is slightly better than the convergent solution by JBD-sec. The regularized solutions by JBD-WGCV gradually converges, but its accuracy is considerably lower than other methods.

From table 4, we find that both the discrepancy principle and the L-curve of form (5.7) give estimated k_0 not too far from the optimal one, and the corresponding

relative errors are only slightly larger than that of x_{k_0}. Therefore, among all these methods, JBD-WGCV is the least accurate method for restored the two test images, while for the JBD based JBDQR and JBD-sec, the reconstructed solutions have at least the same accuracy as that obtained by LSQR.

7. Conclusion. For the JBD based regularization algorithms for solving large scale ill-posed problems, we must solve a large scale inner least squares problem (2.11) at each outer iteration. We investigate the solution accuracy of (2.11) and give some results about the numerical behavior of the joint bidiagonalization process. We show that the solution accuracy of (2.11) can be relaxed considerably while it will not reduce the accuracy of regularized solutions, and the stopping tolerance of LSQR for solving (2.11) can be set as $\tau = \|e\|^2/\|b\|$, thus the overall efficiency of the algorithms can be improved substantially.

We discuss some methods to estimate the optimal stopping iteration k_0 for JBDQR, including the discrepancy principle and the L-curve method, and propose a procedure to update regularized solutions step by step efficiently. For the hybrid method, we give an automatic parameter updating method, called "secant update", which is efficient and robust. Finally we use both one and two dimensional test problems to illustrate our results and show some numerical performance of the JBD based regularization algorithms.

REFERENCES

[1] S. Berisha and J. G. Nagy, *Restore Tools: Iterative methods for image restoration*, 2012. Available from http://www.mathcs.emory.edu/~nagy/RestoreTools.

[2] Å. Björck, *A bidiagonalization algorithm for solving large and sparse ill-posed systems of linear equations*, BIT, 28 (1988), pp. 659-670.

[3] Å. Björck, *Numerical Methods for Least Squares Problems*, SIAM, Philadelphia, PA, 1996.

[4] J. Chung, J. G. Nagy and D. P. O'Leary, *A weighted-GCV method for Lanczos-hybrid regularization*, Electr. Trans. Numer. Anal., 28 (2008), pp.149–167.

[5] J. Chung and A. K. Saibaba, *Generalized hybrid iterative methods for large-scale Bayesian inverse problems*, SIAM J. Sci. Comput., 39 (2017), pp. S24–S46.

[6] J. Chung, A. K. Saibaba, M. Brown and E. Westman, *Efficient generalized Golub-Kahan based methods for dynamic inverse problems*, Inverse Probl., 34 (2018), 024005.

[7] L. Eldén, *A weigthed pseudoinverse, generalized singular values and constrained least squares problems*, BIT, 22 (1982), pp. 487–501.

[8] S. Gazzola, P. C. Hansen, and J. G. Nagy, *IR Tools: a MATLAB package of iterative regularization methods and large-scale test problems*, Numer. Algor., 81 (2019), pp. 773–811.

[9] S. Gazzola and P. Novati, *Automatic parameter setting for Arnoldi-Tikhonov methods*, J. Comput. Appl. Math., 256 (2014), pp. 180-195

[10] G. H. Golub and C. F. van Loan, *Matrix Computations*, 4th ed., The Johns Hopkins University Press, 2013.

[11] P. C. Hansen, *Rank-Deficient and Discrete Ill-Posed Problems: Numerical Aspects of Linear Inversion*, SIAM, Philadelphia, PA, 1998.

[12] ———, *Regularization tools version 4.0 for Matlab 7.3*, Numer. Algor., 46 (2007), pp. 189–194.

[13] ———, *Discrete Inverse Problems: Insight and Algorithms*, SIAM, Philadelphia, PA, 2010.

[14] P. C. Hansen, J. G. Nagy and D. P. O'Leary, *Deblurring Images: Matrices, Spectra and Filtering*, SIAM, Philadelphia, PA, 2006.

[15] N. J. Higham, *Accuracy and Stability of Numerical Algorithms*, 2nd ed., SIAM, Philadelphia, 2002.

[16] I. Hnětynková, M. Plešinger, and Z. Strkoš, *The regularization effect of the Golub-Kahan iterative bidiagonalization and revealing the noise level in the data*, BIT, 49 (2009), pp. 669-696.

[17] Z. Jia, *Approximation accuracy of the Krylov subspaces for linear discrete ill-posed problems*, J. Comput. Appl. Math., 374 (2020), 112786.

[18] ———, *The low rank approximations and Ritz values in LSQR for linear discrete ill-posed*

problems, Inverse Problems, 36 (2020), 045013.

[19] ———, *The Krylov subspace, low rank approximations and Ritz values of LSQR for linear discrete ill-posed problems: the multiple singular value case*, arXiv preprint, arXiv:math.NA/2003.09259v1 (2020)

[20] Z. Jia and H. Li, *A backward error analysis of the Lanczos bidiagonalization with reorthogonalization*, manuscript, (2020)

[21] Z. Jia and Y. Yang, *A joint bidiagonalization based algorithm for large scale linear discrete ill-posed problems in general-form regularization*, arXiv preprint, arXiv:math.NA/1807.08419v2 (2018)

[22] Z. Jia and Y. Yang, *Modified truncated randomized singular value decomposition (MTRSVD) algorithms for large scale discrete ill-posed problems with general-form regularization*, Inverse Problems, 34 (2018), 055031.

[23] J. Kaipio and E. Somersalo, *Statistical and Computational Inverse Problems*, Applied Mathematical Sciences 160, Springer, 2005.

[24] M. E. Kilmer, P. C. Hansen, and M. I. Espanol, *A projection-based approach to general-form Tikhonov regualarization*, SIAM J. Sci. Comput., 29 (2007), pp. 315–330.

[25] M. E. Kilmer and D. P. O'Leary, *Choosing regularization parameters in iterative methods for ill-posed problems*, SIAM J. Matrix Anal.Appl., 22 (2001), pp. 1204–1221.

[26] H. Li, *A rounding error analysis of the joint bidiagonalization process with applications to the GSVD computation*, arXiv preprint, arXiv:math.NA/1912.08505v1 (2019)

[27] J. G. Nagy, K. Palmer, and L. Perrone, *Iterative methods for image deblurring: A Matlab object-oriented approach*, Numer. Algor., 36 (2004), pp. 73–93.

[28] E. Natterer, *The Mathematics of Computerized Tomography*, John Wiley, New York, 1986.

[29] D. P. O'Leary and J. A. Simmons, *A bidiagonalization-regularization procedure for large scale discretization of ill-posed problems*, SIAM J. Sci. Statist. Comput., 2 (1981), pp. 474–489.

[30] C. C. Paige and M. A. Saunders, *LSQR: An algorithm for sparse linear equations and sparse least squares*, ACM Trans. Maths. Soft., 8 (1982), pp. 43–71.

[31] R. A. Renaut, S. Vatankhah, and V. E. Ardesta, *Hybrid and iteratively reweighted regularization by unbiased predictive risk and weighted GCV for projected systems*, SIAM J. Sci. Comput., 39 (2017), pp. B221–B243.

[32] L. Reichel and G. Rodriguez, *Old and new parameter choice rules for discrete ill-posed problems*, Numer. Algor., 63 (2013), pp. 65–87.

[33] P.-Å. Wedin, *Perturbation bounds in connection with the singular value decomposition*, BIT 12 (1972), pp. 99-111.

[34] H. Zha, *Computing the generalized singular values/vectors of large sparse or structured matrix paris*, Numer. Math., 72 (1996), pp. 391–417.